ASTRONOMY & ASTROPHYSICS
SUPPLEMENT SERIES

Astron. Astrophys. Suppl. Ser. **59,** 523-555 (1985)

Time variations and shell sizes of OH masers in late-type stars

J. Herman (*) and H. J. Habing

Sterrewacht Leiden, Postbus 9513, 2300 RA Leiden, The Netherlands

Received July 23, accepted November 6, 1984

Summary. — We present the results of a program in which frequently the flux density of OH masers in late-type stars was measured, to determine the variability, its period and amplitude.
Normal Mira variables have « radio » periods that are equal to their optical periods ($\sim$ 400 days). Most of the related, but optically unidentified OH/IR stars have much longer periods, up to $\sim$ 2000 days. A significant fraction (25 %) of the OH/IR stars shows small amplitude, or no variations.
The light curves of different peaks in the line profile of one star have the same periodicity and shape, but differ slightly in phase. From these phase differences linear dimensions of the OH shells can be derived; typical values for the radii are $\sim 8 \times 10^{15}$ cm for Mira variables and $\sim 5 \times 10^{16}$ cm for OH/IR stars.

Key words : stars : late-type stars — long period variables — masers — circumstellar matter.

1. Introduction.

The last stages of stellar evolution, in the red giant region of the Hertzsprung-Russell diagram, have become an increasingly frequent subject of observational and theoretical studies ever since the infrared and microwave parts of the spectrum have become accessible. Most objects in the 2.2 μm InfraRed Catalogue (IRC; Neugebauer and Leighton, 1969) are late-type giants (see e.g. Bidelman, 1980). The detection of maser emission from molecules such as OH, H_2O, and SiO in these objects (see Engels' catalogue, 1979) was one of the milestones and ultimately led to the discovery of an extreme class of red giants and supergiants : the OH/IR stars (see e.g. Jones *et al.*, 1983; Herman and Habing, 1984). The OH maser line profiles of the OH/IR stars closely resemble those of the strongest masering Mira variables, and this has been the main argument in favour of a relationship between the two classes of objects. Even more convincing would be the establishment of long period variations in the OH/IR stars (in the infrared or in the maser lines), similar to the Mira variables. For that purpose a monitor program was started in 1978 with the 25-m Dwingeloo Radio Telescope, measuring frequently the 1612 MHz line fluxes of strong OH masers. Here the results of the first five years of this program are presented. Preliminary results presented before (Herman and Habing, 1981) are fully superseded by this paper.

The results consist of two kinds : directly measured and inferred quantities. From the light curves one can derive a period, an amplitude, and a mean flux. However, it proved possible to determine in one object light curves for a number of different peaks in the line profile. Schultz *et al.* (1978) predicted that small phase differences exist between light curves of different peaks. For IRC+10011 Jewell *et al.* (1980) demonstrated that such a phase lag indeed is present. These phase differences reflect differences in light traveltime, and are a measure of the linear size of the OH masing shell.

In section 2 the observations are discussed, and in section 3 the general characteristics of the « radio » light curves : periods, amplitudes, shapes. In section 4 we consider the predicted phase differences and a method to derive shell sizes from them. Section 5 contains the results and section 6 a summary.

We are aware of two other publications reporting results comparable to ours : a study of the infrared variability of OH/IR stars by Engels *et al.* (1983), and a study of the OH variability (Jewell *et al.*, 1979). The last study led also to a determination of the OH shell size of IRC+10011 (Jewell *et al.*, 1980).

The results presented in this paper have appeared before in Chapter II of the thesis of one of us (Herman, 1983).

2. Observations : the sample of objects, methods of observation and data reduction.

2.1 Selection of the sample. — The intent of this program was to compare the variability of well known Long Period Variables with that of unidentified OH/IR stars. The sample contained nine Mira variables and three M-type supergiants (VY CMa, PZ Cas, and NML Cyg) with OH maser emission, and all OH/IR stars ($10^o < l < 180^o$) with a harmonic mean flux, $\{ S_L . S_H \}^{1/2} > 4$ Jy

(*) Present address : ESTEC, Postbus 299, 2200 AG Noordwijk, The Netherlands.
Send offprint requests to : J. Herman.

from Baud's catalogue (Baud *et al.*, 1981). Also added were three sources at the galactic centre with large (negative) radial velocities. Thus a total of 60 stars was followed regularly during 4-6 years. Because the telescope was also used for other programs, our coverage has gaps of months to fortnights, but one stretch of over 200 days was covered continuously. About 5000 usable spectra were measured, reduced, calibrated, and plotted with standard programs. For each star we measured the integrated flux and the various peak flux densities. This resulted in 5-20 radio light curves per star.

2.2 OBSERVATIONS. — The observations were made with the 25-m Dwingeloo Radio Telescope (DRT) at a frequency of 1612.231 MHz ($\lambda = 18$ cm). The half power beam width is 31′ at this frequency, the aperture efficiency is 64 %, and $S/T_A = 8.772$ (Jy/K) (Slottje, 1982). The DRT used a closed-cycle helium cooled parametric amplifier and a single linearly polarized feed, replaced in 1982 by a FET amplifier and two linearly polarized feeds. A 256-channel autocorrelation spectrometer was used in the total power mode over a bandwidth of 625 kHz (116 km s^{-1}), yielding a resolution (uniform weighting) of 2.93 kHz, or 0.54 km s^{-1}. The signal was clipped in the one-bit mode. The system temperature typically was 35 K at the beginning of a run, slowly increasing to $\sim$ 40 K after several weeks of observing.

2.3 CALIBRATION. — The system was calibrated continuously against a noise tube of known constant temperature, the noisestep, *NS*. This calibration was checked daily (in principle) by measuring a continuum point source with a known flux. We used Virgo A (189.45 Jy at 1612 MHz) or occasionally Cygnus A (1369.3 Jy; Baars *et al.*, 1977). The noisestep varied less than 1 % over one day in general (see Fig. 1), although some larger deviations occurred, especially during times when the continuum measurements were of poor quality (Murphy's law; see Bloch, 1979). Because a good calibration is important for the determination of the relative phase for the different light curves of one star, we applied in addition an internal calibration, as described in section 2.5.

2.4 DATA REDUCTION. — The off-line reduction was performed with available standard programs, yielding spectra calibrated in antenna temperature. The theoretical noise in the spectra is given by (see Ball, 1976)

$$\Delta T_{\mathrm{RMS}} = \frac{\alpha\gamma\, T_{\mathrm{sys}}}{(1.2\,\beta t)^{1/2}}\,(\mathrm{K}) \qquad (1)$$

where $1 \lesssim \alpha < 2$ for optimum total power, γ is 1.47 for the one-bit mode, β is the channel spacing in Hz, and t is the integration time in seconds. Integration times ranging from 120 to 7200 s were used, leading to $\Delta T_{\mathrm{RMS}} = 0.15 - 0.019$ K. This is in reasonable agreement with the noise measured in the emission-free parts of the band, except at smaller galactic longitudes where confusion and background radiation can enhance the noise by a factor 2 (see Fig. 2). In our analysis always the measured values of the noise were used.

2.5 INTERNAL CALIBRATION. — In general the calibration is good to within 1-2 %. On some days, however, no calibration measurement was made at all, or the measurement was ruined by interference or by other causes. In those cases the spectra were scaled with the noisestep from another day. With an « internal » calibration procedure the interpolations can be checked, and possibly corrected. It can also serve to find out whether the noisestep, being nearly constant from day to day, has larger deviations on shorter timescales. In each calibration interval some 10-20 sources were observed. For all these one can determine the (relative) residuals with respect to the sinewave as calculated in section 3.3 (Eq. (7)). So for each star, i, with k peaks measured at Julian Day, JD(i), within a certain calibration interval, there are k residuals

$$\mathrm{Res}_k(i) = \{\, S_k(i) - \mathit{Comp}_k(i) \,\}/S_k(i) \qquad (2)$$

where $S_k(i)$ is the measured flux density of peak k, and $\mathit{Comp}_k(i)$ the calculated value (Fig. 3). And although an individual star may show systematic deviations from a sinewave, for a sample it is a perfect representation and the sum of the residuals should be zero in each calibration interval. Now let N be the number of sources in a particular interval. Then the weighted sum of the residuals, α, is

$$\alpha = \frac{\sum_{i=1}^{N}\left[w(i) \sum_k \{\, w_k \log (1 - \mathit{Res}_k(i)) \,\}\right]}{\sum_{i=1}^{N} w(i) \sum_k w_k} \qquad (3)$$

where $\sum_k \{ \ldots \} \Big/ \sum_k$ is a weighted mean of the residuals for the individual peaks and $\sum_i [\ldots] \Big/ \sum_i w(i)$ a weighted mean over all sources in the calibration interval. The statistical weights include the number of peaks per star and the signal-to-noise ratio per peak. Clearly $\alpha = 0$ only if the calibration was correct. The distribution of α-values is shown in figure 4. It shows that the overall calibration is good, but some larger deviations occur, mostly (as expected) when no calibration measurement was made at all. The few days with a deviation > 15 % include the three runs (on 11 stars only) in 1976 and 1977 during Baud's survey. This may be explained by a number of (minor) changes in the receiver system and in the noise tube temperature that where introduced after that survey.

All flux densities were adjusted with the correction factor 10^{α} in the appropriate interval. There is no indication of a systematic variation of α with time within any calibration interval.

2.6 CONFUSING SOURCES. — Because of the large beam (31′) of the DRT, and the crowding of OH/IR stars in the region $l = 10^{\circ}$ to 35° (Baud *et al.*, 1981), we were troubled by confusion in several cases. Table I lists these program stars and describes the influence of the confusion.

Confusion mostly affected the integrated flux densities, due to the uncertainties in the baselines. The peak fluxes are only mildly afflicted, except for the worst cases (see Fig. 5). The time behaviour enabled us to select the features belonging to the program stars.

3. Light curves : periods, amplitudes, asymmetries.

3.1 THE SHAPE OF A LINE PROFILE. — In this section the most conspicuous properties of the (irregularly) sampled light curves are discussed : the periods, the amplitudes, and asymmetries. As a side product of our detailed measurements the expansion velocity of the OH shells is found more accurately than before.

First a description of a typical line profile is given. OH/IR stars characteristically have spectra dominated by two peaks with a separation of 20-40 km s^{-1}, steep outer edges, and a more gradual decline between these peaks (Fig. 6). This shape of the spectrum can be explained if the maser emission comes from a rather thin, uniformly expanding shell (Reid *et al.*, 1977). In this picture the strongest maser emission originates from the front and from the back sides of the shell, where the gain pathlength along the line of sight is longest (see Fig. 13 for a graphical display). The separation between the outer peaks is twice the expansion velocity of the shell; the stellar velocity lies halfway between the peaks. There is a lot of evidence in support of this model which will be summarized in another paper (Herman and Habing, 1984).

On a number of Julian Days, JD(i) (where $30 < i_{\rm total} < 150$), we measured for each star the total range of emission, $\delta v(i)$; the stellar velocity, $v_*(i)$; and the velocity, peak flux density and full width at half maximum for a total of $k_{\rm T}$ recognized peaks (each indicated by the subscript k), $v_k(i)$, $S_k(i)$ and $fw_k(i)$ (where $2 \leqslant k_{\rm T} < 20$). We integrated the flux density over two equal halves of the spectrum yielding the low- and high-velocity integrated flux density, $S_{\rm LV}(i)$ and $S_{\rm HV}(i)$. Finally the noise, $\Delta T_{\rm RMS}(i)$, was determined from an emission-free part in the band. These are the input data for further analysis.

3.2 EXPANSION VELOCITIES. — The expansion velocity of the OH shell is an important, and directly measurable quantity. Usually the expansion velocity ($v_{\rm e}$) has been taken as half the separation between the two strongest peaks in the line profile ($\frac{1}{2}\Delta v$), but here a somewhat different method is adopted. In each of the spectra the total range (δv; see Tables IIa, b) of emission is measured and compared with the velocity separation of the two outermost (not necessarily the strongest) peaks in the spectrum ($\Delta v'$) (see Figs. 7a and 7b). We find, defining $v_{\rm e} \equiv \frac{1}{2}\Delta v'$, with our velocity resolution of 0.54 km s^{-1}

$$v_{\rm e} = \frac{1}{2}\{\,\delta v - 2.55\,\}\ ({\rm km\ s^{-1}})\,. \qquad (4)$$

This expression is valid for all 1612 MHz OH emitters.

That equation (4) holds from the smallest Δv's (the OH-Mira's) to the largest (the supergiants) tells us that the physical conditions in the masing regions are for all sources more or less the same.

3.3 PERIOD AND AMPLITUDE DETERMINATIONS. — To determine periods and amplitudes a sinewave function is fitted to the observed flux densities by least squares, weighted with the measured RMS noise. For each star this resulted in $k_{\rm T} + 2$ light curves, for $k_{\rm T}$ peaks and for the integrated flux densities, each having four degrees of freedom (the mean flux density a_k, the amplitude b_k, the time of maximum $\underline{\rm JD}_{k_0}$, and the period P_k)

$$S_k(i) = \underline{a}_k + \underline{b}_k \cos\left[2\pi\,\{\,{\rm JD}(i) - \underline{\rm JD}_{k_0}\,\}/P_k\right]. \qquad (5)$$

It is known (Harvey *et al.*, 1974) that (optically identified) OH masers vary nearly in phase with their optical or infrared counterparts with a fixed amplitude ratio between the wavelength regimes. This indicates that the masers are radiatively pumped by the central star and are saturated. If this situation is also true for the unidentified OH/IR stars, the period (P_k) and the relative amplitude ($B_k \equiv b_k/a_k$) are expected to be the same for all peaks in the spectrum of one star. Our results show that this is indeed the case (Figs. 8a and 8b). Furthermore, for some OH/IR stars Engels *et al.* (1983) determined light curves in the infrared, yielding the same periods and phases as the radio light curves. Measurements by Feast (private communication) also confirm the coupling between IR and radio (see Herman, 1983). This result supports a further step : we demand the period and relative amplitude to be constant for a given source. At this point it is good to note that the fact that the relative amplitude is the same for all curves of one star, naturally leads to the introduction of radio magnitudes, $m_k \equiv \log S_k$, instead of flux densities. From section 3.4 onward these will be used in the more detailed discussion of the light curves : their shapes and their small phase differences.

The period, P, and the relative amplitude, B, of a star were calculated by taking the mean over all curves, weighted by the quality of the sinewave fit and the strength of the feature. Thus

$$P = \sum_k P_k\, w_k \Big/ \sum w_k\,, \quad \text{and} \quad B = \sum_k \frac{b_k}{a_k}\, w_k \Big/ \sum w_k \qquad (6)$$

where the summation is over $k_{\rm T}$ peaks and over the low- and high-velocity integrated flux. Again a sinewave is fitted to the flux densities, but this time one with only two degrees of freedom (the mean flux a_k and the time of maximum $\underline{\rm JD}_{k_0}$)

$$S_k(i) = \underline{a}_k\,\{\,1 + B\cos\left[2\pi\,\{\,{\rm JD}(i) - \underline{\rm JD}_{k_0}\,\}/P\right]\,\}\,. \qquad (7)$$

Tables IIa and IIb give the results for all program stars.

3.4 ASYMMETRY OF THE RADIO LIGHT CURVES. — In general the visual light curves of Mira variables are asymmetric (see e.g. Campbell, 1955), but the asymmetry, usually expressed as $f \equiv (m - M)/P$, the fraction of the period between minimum and maximum, becomes less pronounced at longer wavelengths (Lockwood and Wing, 1971). It is known that Mira variables with smaller f-values, i.e. a steep rise to maximum and a more gradual decline to minimum, are more likely to show maser emission (Bowers and Kerr, 1977). Although the radio light curves reflect the variation at long IR wavelengths (35 μm; Elitzur, 1981), inspection of our curves for the OH/IR stars revealed clear, systematic deviations from a sinewave function. As noted in section 3.3 it makes sense to use radio magnitudes, $m_k(i) \equiv \log S_k(i)$, in the further analysis. The subscript k assumes the values 1, 2, ..., $(k_{\rm T} + 2)$ for a star with $k_{\rm T}$ peaks by including the low- and high-velocity integrated flux density.

Define

$$\phi_k(i) = \{ \mathrm{JD}(i) - \mathrm{JD}_{k_0} \}/P \quad (8)$$

where P and JD_{k_0} are taken from section 3.3. Now an asymmetric lightcurve is fitted to the datapoints by matching two segments of different sinusoids with the same amplitude, but different period

$$m_k(i) = m_{0k} + m_{1k} \cos \{ 2\pi\phi_k(i)/2f_k \} \quad (9a)$$

for $\phi_k(i) > 1 - f_k$ (ascending branch), and

$$m_k(i) = m_{0k} + m_{1k} \cos \{ 2\pi\phi_k(i)/2(1 - f_k) \} \quad (9b)$$

for $\phi_k(i) < 1 - f_k$ (descending branch).

Again two steps are taken : in the first four unknowns are solved (m_{0k}, m_{1k}, ϕ_k, and f_k), although the mean flux $m_{0k} \simeq \log \{ (1 + B)/(1 - B) \}$ can differ only marginally from the values as found in section 3.3. In the second step m_1 and f are demanded to be the same for all $(k_T + 2)$ light curves of a given star. As before the mean values over the $(k_T + 2)$ curves are used, weighted with the strength of the feature and the quality of the fit. The numerical results can be found in table III ; the radio curves in appendix A (Figs. 1-59).

4. Phase differences and shell radii.

4.1 Predicted effects. — Estimates of the OH shell radii give typically $\sim 10^{16}$ cm, or 4 light days. In a simple model (e.g. Reid *et al.*, 1977) twice this light travel time is expected as difference between the variations of the high-velocity (back), and low-velocity (front) peak in a 1612 MHz line profile (see Fig. 13). Compared to the period of variation, the time difference is small, but with a sufficient sampling of the light curves it is measurable. Statistically, such phase shifts were demonstrated to exist by Schultz *et al.* (1978), and convincingly found for IRC + 10011 by Jewell *et al.* (1980). One of the major goals of our program, from its start in 1978, has been the measurement of these phase differences for as many stars as possible.

A simple model to describe the effects quantitatively is shown in figure 13 (see also Herman, 1983) ; the following equations go with this figure

$$v_r = - v_e \cos \psi \quad (10)$$

where v_e is the expansion velocity of the shell, v_r the radial velocity in the rest frame of the star, and ψ the angle between the direction of expansion and the line of sight. In this notation $v_r(\psi) < 0$ for $-\frac{\pi}{2} < \psi < \frac{\pi}{2}$. Also

$$x = R \{ 1 - \cos \psi \} = R \left\{ 1 + \frac{v_r}{v_e} \right\}. \quad (11)$$

The quantity x/c is the time difference between the variation of the « front » peak (in phase with the star) and the peak k at v_{rk}. Clearly the time difference is largest, with the value $2\,R/c$, between the front peak ($v_{rf} = - v_e$) and the back peak ($v_{rb} = + v_e$). The general expression for the phase difference with an arbitrarily chosen peak j as the phase reference becomes

$$\Delta\phi_{kj} = \frac{R}{cv_e P} \{ v_{rk} - v_{rj} \}. \quad (12)$$

Because all other quantities in equation (12) are measurable, R, the radius of the OH shell can be determined.

The phase difference between the light curves for the integrated flux densities can also be used

$$\Delta\phi(\mathrm{HV} - \mathrm{LV}) \simeq 0.8 \frac{2\,R}{cP} \quad (13)$$

(see for the derivation of this equation : Herman, 1983).

4.2 Considerations on the method of analysis. — The determination of $\Delta\phi$, and hence of R, is less straightforward than that of the period or the amplitude of the light curve, because it is such a small quantity. The times of maximum of the light curves of each star have been found in section 3.3 (Eq. (7)) with a typical accuracy of 5 % of the period. This is also the magnitude of the expected phase delay. Thus to find $\Delta\phi$ another approach is needed, which will be a differential method.

For a given star flux density measurements have been taken at irregularly spaced phases, ϕ_i. These sample the light curves for several peaks, labelled j and k. In this notation k is the running index, $k = 1, \ldots, k_T$, and j denotes the feature chosen as the phase reference. Now write for the radio magnitudes (see Eq. (9) ; Sect. 3.4)

$$m_j(\phi_i) = m_{0j} + \Delta m'\, g(\phi_i) \quad (14a)$$

$$m_k(\phi_i) = m_{0k} + \Delta m'\, g(\phi_i + \Delta\phi_{kj}) \quad (14b)$$

where, as before, it is assumed that $\Delta m'$ (here defined as $0.2\,\Delta m_r$, the values listed in table II), and g, an arbitrary periodic function that describes the light curve to the nth degree, are the same for all curves of one star.

Because $\Delta\phi_{kj}$ is expected to be a small quantity, we expand equation (14) in a Taylor series and find

$$[m_k(\phi_i) - m_{0k}] - [m_j(\phi_i) - m_{0j}] = \Delta m' \{ \Delta\phi_{kj}\, g'(\phi_i) + \tfrac{1}{2} \Delta^2\phi_{kj}\, g''(\phi_i) + \cdots \}. \quad (15)$$

There are two different ways to find $\Delta\phi_{kj}$ from this equation.

(a) Determine g and its derivatives and then, because all other quantities are measurable, $\Delta\phi_{kj}$ follows. Jewell *et al.* (1980) took a sinewave function for g, and used equation (15) to the first order to find $\Delta\phi_{kj}$. This approach is less attractive, because any deviation from the assumed shape of g will produce a systematic error in the estimate of $\Delta\phi_{kj}$, that will not be suppressed by going to higher order approximations. But in principle any irregularity in the light curves, such as humps, secondary maxima, or a steep rise to maximum, contributes to a *better* determination of the phase shift.

(b) Assume that the mean fluxes, m_{0k} and m_{0j}, can be determined and leave $\Delta m'$ and g completely free. Now displace each curve k over a certain phase shift, ε, and correlate its values with those of the unshifted curve j. That is, by interpolation one can estimate $m_k(\phi_i + \varepsilon)$ for various values of ε, and determine that value for which

$$\sum_i \{ [m_k(\phi_i + \varepsilon) - m_{0k}] - [m_j(\phi_i) - m_{0j}] \}^2 \quad (16)$$

reaches a minimum. That value of ε is $\Delta\phi_{kj}$.

4.3 IMPLEMENTATION OF THE CORRELATION ANALYSIS. — The correlation analysis, method (b) in section 4.2, was implemented in the following manner. For all k curves (also for $k = j$) of a star the radio magnitudes, m_k, were calculated at a set of « normal phase points » $\phi_l = l.\varepsilon$. $\varepsilon = 0.002$ is an incremental phase step, and $l = 1, 2, ..., 500$. For each calculation observed values $m_k(\phi_i)$ were selected where $|\phi_i - l.\varepsilon| < 0.05$; $m_k(\phi_i)$ was multiplied by $\cos(l.\varepsilon)/\cos(\phi_i)$ ([1]), and then a weighted mean of all values m_k within the interval was taken. This weight was a product of two factors : the signal-to-noise ratio and $|\phi_i - l.\varepsilon|^{-1}$. For some normal points there is no value of $m_k(\phi_i)$ available within 0.05 phase. So, each calculated value, $m_k(l.\varepsilon)$, is assigned a weight, $t_k(l.\varepsilon)$, equal to the number of measured points in the interval, $l.\varepsilon \pm 0.05$.

Now the light curves are given at regularly spaced phase points, $l.\varepsilon$, a quantity $R_{kj}(l, \Delta l)$ can be defined

$$R_{kj}(l, \Delta l) = \{ m_k(l.\varepsilon + \Delta l.\varepsilon) - m_{0k} \} - \{ m_j(l.\varepsilon) - m_{0j} \} \quad (17)$$

where $\Delta l = -80, -79, ..., 79, 80$. It is obvious that $R_{kj}(l, \Delta l) \to 0$ if $\Delta l.\varepsilon \to \Delta\phi_{kj}$, provided that $m_k(\phi_i)$ was sampled often enough, and measured with sufficient accuracy. Because both conditions are restricted by profane reasons, $\Delta\phi_{kj}$ is determined by minimizing

$$\sigma_{kj}(\Delta l) \equiv \sum_{\substack{l=1 \\ t_k \neq 0 \\ t_l \neq 0}}^{500} \{ R_{kj}^2(l, \Delta l) [t_k(l.\varepsilon + \Delta l.\varepsilon) + t_j(l.\varepsilon)] \} / \sum_{l=1}^{500} \{ t_k(l.\varepsilon + \Delta l.\varepsilon) + t_j(l.\varepsilon) \}. \quad (18)$$

5. Results.

For the identified stars (see Table IIa) the variable star name, the IRC number and the AFGL number are given. The period (P_r) and the amplitude ($\Delta m_r \equiv 2.5 \log \{ S_{max}/S_{min} \}$) as determined from the radio light curves, compared with the optical period (P_0) and amplitude (Δm_v), the stellar velocity (v_* with respect to the Local Standard of Rest) and the total range of emission (δv) are tabulated with their uncertainties. Columns 12 and 11 give the number of observations and the time interval in which they were made. Most observations were made from April, 1980 till October, 1982; 20 sources have been followed regularly from 1978 onward, and for 11 stars three runs, carried out in 1976 and in 1977, were also added. In the last two columns references can be found, containing information about the star and an indication if IR and/or VLA measurements are known to us.

For the OH/IR stars (see Table IIb) the same quantities are listed, when they are known; if a second period is quoted it is an IR period from Engels *et al.* (1983). The OH/IR stars marked by a + sign form a homogeneous sample from Baud's catalogue (Baud *et al.*, 1981), with a harmonic mean flux > 4 Jy.

([1]) In fact, equation (9) was used, taking into account the asymmetry of the curve also.

5.1 DISCUSSION OF THE PERIODS AND AMPLITUDES. — The first thing to note in table IIb (see also Fig. 9) is that the entries can be separated into two groups : variable and non-variable stars. From our homogeneous sample six objects show virtually no variations larger than the 3 σ level : OH 15.7 + 0.8 ($\Delta m_r = 0^m.13$), OH 31.0 − 0.2 ($\Delta m_r = 0^m.13$), OH 37.1 − 0.8 ($\Delta m_r = 0^m.13$), OH 51.8 − 0.2 ($\Delta m_r = 0^m.16$), OH 53.6 − 0.2 ($\Delta m_r = 0^m.12$), and OH 77.9 + 0.2 ($\Delta m_r = 0^m.19$). Except for OH 31.0 − 0.2, none of these sources is disturbed by confusion. Six others have small amplitude variation, that might be periodic. But in these cases our sensitivity is too low, mostly due to confusion, to give a definite answer. These six are : OH 11.5 + 0.1 ($\Delta m_r = 0^m.23$), for which we see no variation in the (very weak) low velocity part of the spectrum, but clear variations in the (much stronger) high velocity peaks. It is impossible to decide whether this behaviour is intrinsic to OH 11.5 + 0.1, or whether it comes from the underlying spectrum of OH 11.3 + 0.0; OH 17.7 − 2.0 ($\Delta m_r = 0^m.16$), a strong OH-emitter with some long term variation; OH 18.3 + 0.4 ($\Delta m_r = 0^m.27$), whose spectrum is completely confused with that of OH 18.3 + 0.1; OH 18.5 + 1.4 ($\Delta m_r = 0^m.19$), that has one or two weak peaks outside the mean velocity range present in about 50 % of the spectra; OH 25.1 − 0.3 ($\Delta m_r = 0^m.21$), which is seriously disturbed by confusion of OH 24.7 − 0.1 in the weaker features and the integrated flux density, but which shows reasonable variation in the two strongest peaks; and OH 31.0 + 0.0 ($\Delta m_r = 0^m.13$), that is associated with W43 in position, but not in velocity and so may be a pre-mainsequence object, showing irregular and (relatively) short term variations. OH 31.0 + 0.0 also has the smallest Δv (19.3 km s^{-1}, cf. $\langle \Delta v \rangle = 30$ km s^{-1}) of all OH/IR stars in our sample and has all of its flux confined to the *VLBI* hotspots (Reid *et al.*, 1977). We can conclude for our sample of 44 OH/IR stars (OH 31.0 + 0.0 omitted) that *14 % do not vary at all, 11 % have such a small amplitude variation that it is hardly recognized with our beam and sensitivity, and that the remaining 75 % vary with amplitudes comparable to those of the nearby, and weak, OH Mira stars.* Note that for the optically identified masers small amplitudes correspond to large Δv, i.e. to the supergiants, but that for the OH/IR stars the « non »-variables are distributed over all Δv ! Finally we note that the three galactic centre sources are constant within their 2 σ uncertainties.

The periods of the OH/IR stars are much longer than the periods of the Mira variables (Fig. 10). For a number of stars our time base is too short, or our phase coverage too incomplete. Although recent, not yet included, observations (1983 and 1984) confirm the tabulated periods, still the maximum might not yet have been observed for OH 21.5 + 0.5, OH 30.1 − 0.7, OH 127.9 + 0.0, and OH 138.0 + 7.2; for OH 75.3 − 1.8 and OH 104.9 + 2.4, we might not have observed the minimum light. OH 17.4 − 0.3 suddenly became a factor 3 stronger at the end of 1983.

5.2 INDIVIDUAL STARS - SPECIAL COMMENTS.

5.2.1 *R Aql and U Ori.* — For all Mira variables period and amplitude change from cycle to cycle, but for most of them these changes are small. In general, observations from different cycles could be combined easily, except for R Aql and U Ori. These will be discussed in some detail.

R Aquilae. — Of the Mira variables in our sample a systematic behaviour of the period with time is known only for R Aql. A reanalysis of the observations of visual maxima during 126 years gives for the times of maximum, t_n, and the period, P_n, as a function of the cycle, n (*cf.* Schneller, 1963)

$$t_n(\max) = 2422301.8 + 312.35\,n - 0.2330\,n^2 + \\ + 0.00045\,n^3 \quad (19a)$$

(Julian Days)

$$P_n = \frac{dt_n}{dn} = 312.35 - 0.4660\,n + 0.00135\,n^2 \text{ (days)} . \quad (19b)$$

The tabulated optical period is for cycle $n = 73$, which corresponds to the middle of our radio observations. Omission of the uncertain second order term in equation (19b) brings the extrapolated period down to 278.3 days, in good agreement with the radio period and the recently determined IR period of 280 days (Rudnitskij, private communication; see also Engels *et al.*, 1983). R Aql has two weak features, at − 6.16 and − 3.72 km s^{-1} (Table III), the first is usually the stronger of the two. In cycle 75-76 (J.D. 244 4700-5100) the relative strength situation was reversed.

U Orionis. — This star flared in 1974 in the 1612 MHz line and since then its flux declined more or less regulary (see Fig. 11). We can write for the total integrated flux density, $S_{TOT} = S_{LV} + S_{HV}$

$$S_{TOT} = 0.749 + 0.251 \cos[\{ JD(i) - JD_0 \}/P] \times \\ \times \exp[3.700 - 0.318\,\{ JD(i) - JD_0 \}/P] \quad (20)$$

where S_{TOT} is in 10^{-22} W m^{-2}, the period $P = 406.3$ days and $JD_0 = 244\,2152$ corresponding to the year 1974.288. Note that the period shows irregularities too. From 1981 on only the two strongest peaks (at $v = -2.92$ and 2.63 km s^{-1}; Table III) remain observable. The two weaker peaks outside have disappeared completely (see also Jewell *et al.*, 1981), and since mid 1982 the 2.63 km s^{-1} feature has also become invisible for the DRT ($S \lesssim 0.25$ Jy, 2 σ).

5.2.2 *Supergiants.* — M-type supergiants can show drastic changes in behaviour; years of quiescence are followed by periods of (semi) regular variation. VY CMa hardly shows any long term variation in the OH emission, but PZ Cas and NML Cyg do, although the amplitudes are small (see also Harvey *et al.*, 1974). However, all three supergiants have large changes in OH flux (PZ Cas > 3 σ; VY CMa and NML Cyg > 5 σ) on timescales of days (see Fig. 12). This is probably caused by the fact that for some spectral features a large fraction (> 50 %) of the power comes from extremely small (< 0".18) maser hotspots (Benson and Mutel, 1979), that are not completely saturated. In Mira variables this fraction usually is ≪ 10 % (Reid *et al.*, 1977), as it is for OH/IR stars (Bowers *et al.*, 1980). If individual spectral features can be identified with these hotspots then observations of the supergiants with high time-resolution can give good estimates of the distances for these objects, when combined with *VLBI* experiments. A rough estimate for VY CMa gives a light travel time across the hotspot associated with the strongest peak in the spectrum (v_k = − 30.17 km s^{-1}; Table III) of $\lesssim 2$ days. When combined with the angular size of $\lesssim 0''.18$, a distance of ~ 1.9 kpc is found, reasonably close to the literature value of 1.5 kpc (Herbig, 1969). The dimension of the hotspot (2 days corresponds to 5×10^{15} cm) indicates that the maser is only partially saturated (*cf.* Goldreich and Keeley, 1972). This could be an important tool in the problem of the distance determination to these objects. For example, NML Cyg is at 500 pc according to Hyland *et al.* (1972), but at 2 kpc according to Morris and Jura (1983).

5.3 DIRECTLY INFERRED QUANTITIES : VELOCITIES, FLUXES AND PHASES. — The following quantities are listed in table III : the name of the star; its period, with below the period the time of maximum for the low velocity integrated flux density ($JD_0 - 2440000$); the f-value (= rise time/period); the amplitude of the sinewave function ($m_1 = 0.2\,\Delta m_r$, from Eqs. (9a) and (9b)); the logarithm of the mean low- and high-velocity integrated flux density ($\log \bar{S}_{LV}$ and $\log \bar{S}_{HV}$); the mean error (1 σ) for an individual measurement (*me*); the phase lag $\Delta\phi$(HV − LV) and its uncertainty; the velocities of all peaks (v_k measured with respect to the stellar velocity v_*); the full width at half maximum (fw_k), if measurable; the logarithm of the mean flux density ($\log \bar{S}_k$); the mean error for an individual measurement (me_k); the phase lags ($\Delta\phi_k$ measured with respect to the given phase zeropoint JD_0) and their errors. The uncertainties in the velocities are not tabulated, but they are usually small (~ 0.03 km s^{-1}; see Tables IIa and IIb). Sources for which $m_1 \lesssim$ (2-3) me_k (depending on the number of observations) are classified as non-variable. Their « periods » are given between parentheses and no phase lags are tabulated. Although the actual errors are larger, the periods and the phase zeropoints are given to 0.1 day accuracy, because the phase lags have accuracies of $\sim 10^{-3}$ P. The radio light curves can be found in Appendix A (Figs. 1-59).

5.4 MODEL DEPENDENT QUANTITIES : SHELL SIZES. — The model of a uniformly expanding shell predicts a linear relation between $\Delta\phi_k$ and v_k

$$R_p = cP\,\Delta\phi_k \left\{ 1 + \frac{v_k}{v_e} \right\}^{-1} . \quad (12')$$

This prediction can be tested by plotting $\Delta\phi_k$ against $\{ 1 + v_k/v_e \}$. The graphs are shown in Appendix B (Figs. 1-51). A least squares fit to equation (12') gives the radii (R_p), while the spread around the slope, R_p/cP is an indication of the applicability of the model, or in other words denotes the uncertainty in the derived value for the radius (ΔR_p). The phase lag between the curves for the high- and low-velocity integrated flux density, $\Delta\phi$(HV − LV), can also be used in order to find a radius, but only if there was no confusion in the spectrum by another source

$$R_i' = \tfrac{1}{2}\,cP\,\Delta\phi(\text{HV} - \text{LV})\,f_c^{-1} \quad (13')$$

where f_c is a correction factor that matches the « integrated » and « peak » radii (see Herman, 1983). The notation R_i' is to make the distinction with the uncorrected radius, $R_i = \frac{1}{2}\,cP\,\Delta\phi$, as plotted in figure 14. Finally, denoting the uncertainties in the found radii as ΔR_p and

$\Delta R_i'$ resp., we calculate R_0 and ΔR_0, the best values for each star, as follows

$$R_0 = \left\{ \frac{R_p}{\Delta R_p^2} + \frac{R_i'}{\Delta R_i'^2} \right\} \left\{ \frac{1}{\Delta R_p^2} + \frac{1}{\Delta R_i'^2} \right\}^{-1} \quad (21a)$$

and

$$\Delta R_0 = R_0 \left[\left\{ \frac{1}{R_p^2} + \frac{1}{R_i'^2} \right\} \left\{ \frac{1}{\Delta R_p^2} + \frac{1}{\Delta R_i'^2} \right\}^{-1} \right]^{\frac{1}{2}} \quad (21b)$$

R_p, R_i', and R_0 are tabulated with their uncertainties in tables IVa-IVd together with the name of the star, the radio amplitude (Δm_r), the expansion velocity (v_e), the mean phase distance between the measured flux points ($\delta\phi$), and the correction factor (f_c), that matches the « integrated » and « peak » radii. Consecutively, different groups of stars are discussed.

OH-Mira's. — Except for WX Ser, all Mira variables show positive correlation between v_k and $\Delta\phi_k$, implying that the simple shell model gives an adequate description of the geometry, although the uncertainties and the deviations for individual features in the spectrum of a star are large. We find for the OH-Mira's a mean value $\langle R_0 \rangle \pm \langle \Delta R_0 \rangle = 0.78 \pm 0.66$ (10^{16} cm), where $\langle \Delta R_0 \rangle$ denotes the average over the tabulated uncertainties, $\Delta R_0 \cdot \langle R_0 \rangle = 0.78 \times 10^{16}$ cm corresponds to a typical phase lag of 6 days. In other words, a sampling rate of at least once per 0.014 (phase) is needed ($P \simeq 400$ days), preferably over one cycle. Comparing this with the tabulated $\delta\phi$'s, and remembering that our coverage was not uniform and that we combined several cycles, we see that we are unable to decide whether the deviations from the expanding shell model are intrinsic, or are caused by the uncertainties.

Supergiants. — The supergiants VY CMa and NML Cyg have small amplitude long term variations, but show large, random variations on time scales of days. There is some correlation between v_k and $\Delta\phi_k$, but just reversed with respect to the Mira variables and OH/IR stars. This means either that the geometry of the supergiants is different, or that they have large random velocities. We should bear in mind, however, that our method of determining the phase lags is based on the assumption that the variation of the different features are correlated (i.e. complete saturation and radiative pumping). This assumption might be in error for these stars.

OH/IR stars with large amplitudes. — All OH/IR stars with large amplitudes ($\Delta m_r > 0^m.60$) obey the expanding shell model with rather small deviations (~ 20 %). We find a mean value $\langle R_0 \rangle \pm \langle \Delta R_0 \rangle = 5.46 \pm 0.91$ (10^{16} cm), considerably larger than for the OH-Mira's. This gives an intrinsic OH-luminosity (see Herman and Habing, 1984) ~ 300 times larger than the Mira's, if the conditions are the same. This conclusion is in good agreement with that by Baud and Habing (1983).

OH/IR stars with small amplitudes. — For the OH/IR stars with smaller amplitudes an increasing number of sources show a negative, i.e. non-physical, correlation between v_k and $\Delta\phi_k$. For $0^m.30 < \Delta m_r < 0^m.60$ these are 5 out of 12, and for $\Delta m_r < 0^m.30$ 3 out of 6 objects. In all cases a positive value for R_0 is within the uncertainties. The mean value for the small amplitude stars ($\Delta m_r < 0^m.60$) is $\langle R_0 \rangle \pm \langle \Delta R_0 \rangle = 3.75 \pm 1.62$ (10^{16} cm). For all OH/IR stars that are variable $\langle R_0 \rangle \pm \langle \Delta R_0 \rangle = 4.85 \pm 1.16$ (10^{16} cm) is found (see Figs. 14 and 15). With a mean period of ~ 1000 (days) it demands a coverage of at least once per 0.036 (phase) to determine the phase lag with sufficient accuracy. This condition is satisfied by almost all sources (see $\delta\phi$, Table IV). Furthermore, we did not have to combine more cycles for the OH/IR stars, so avoiding larger uncertainties due to irregularities in amplitude and length of the period in successive cycles.

It is interesting that as well for the Mira's as for the OH/IR stars the numerical value of the uncertainty in radius is ~ 10^{16} cm. In another paper (Herman *et al.*, 1984a) it will be shown that the spread in the relation between $\Delta\phi_k$ and v_k is correlated with the deviations from spherical symmetry, or with the thickness of the shell, and also with the flux ratio of the « front » and « back » peaks. The implication is that all stars in our sample have OH shells ~ 10^{16} cm thick. This is in good agreement with theoretical calculations (Elitzur *et al.*, 1976) that predict a saturated maser for an OH column density of ~ 10^{17} cm^{-2} with a nominal density $n_{OH} \simeq 3$ cm^{-3}. If $\langle \Delta R_0 \rangle$ indeed reflects the thickness of the shell, this sets a limit to the accuracy that can be obtained in the determination of R_0, at least as long as a simple model is used. Based on the peak ratio (see Herman and Habing, 1984) this limit is found to be ~ 40 % for the Mira variables and $\lesssim$ 20 % for the OH/IR stars.

We conclude that reasonable and consistent results were obtained for the OH-Mira's, determining radii for 8 of them (out of 9) to ~ 50 % accuracy. For the homogeneous sample of 44 OH/IR stars radii were found for 29 down to ~ 10 % accuracy. For 9 stars (including NML Cyg), all with small amplitude variations, the accuracy was too low to allow the determination of a phase lag. Six OH/IR stars did not vary at all (see Table IVe).

6. Conclusions and summary.

It is possible to study the time behaviour of strong 1612 MHz OH-masers ($S_H > 4$ Jy) with a relatively small telescope, although confusion is a serious problem in those regions where the OH/IR stars are close to one another in the sky and in velocity. To obtain reliable periods it is necessary to follow these sources for several years. The length of our program (3-5 years) proved to be too short for the longest periods ($P \sim 2000$ days). Furthermore, for most OH/IR stars only one cycle was covered, so that we are unable to say whether or not *l'histoire se répète*. Comparison with older observations (e.g. Wilson and Barrett, 1972; or Harvey *et al.*, 1974) indicates that on the longest timescales now available (over 10 years) the radio light variations do repeat, although the same enigmatic changes in the length of the period and in the strength of the maxima may occur as displayed in the optical by the normal Mira variables. The radio amplitudes of the OH/IR stars are comparable to those of the OH-Mira's, but also a number of OH/IR stars was found with small amplitude and irregular variation as is charac-

teristic of supergiants. Their expansion velocities, however, are much smaller than expected for supergiants.

The phase differences between the various curves of one star gave us a good determination of the shell radius for the OH/IR stars ($\sim 5 \times 10^{16}$ cm), provided that we had good coverage of either the maximum or the minimum in the light curve. The OH-Mira's, having much smaller sizes ($\sim 8 \times 10^{15}$ cm), require a sampling rate of at least once per 6 days. Because they are weak OH-emitters and because the Dwingeloo telescope is rather small, in practice this means even more frequent observing. The combination of several cycles does not seem to increase the accuracy of the phase lags by the expected amount, due to the poor reproducibility of the phase and the amplitude of the variation.

The deviations from the simple model of a uniformly expanding shell give an impression of the thickness of the shells. This is found to be $\sim 10^{16}$ cm, of the same order of magnitude as the shell radius for the OH-Mira's, and $\sim 20\,\%$ of the radius for the OH/IR stars. The finite thickness of the OH shells actually limits the applicability of phase lag measurements in order to determine radii of the circumstellar envelope.

Acknowledgements.

We thank B. Baud for many useful comments, and P. Bles for doing part of the reduction. M. W. Feast kindly provided us with infrared data on a number of OH Mira variables. This work was supported by a grant from ASTRON, the Netherlands Foundation for Astronomical Research. The Dwingeloo Radio Telescope is operated by S.R.Z.M., the Netherlands Foundation for Radio Astronomy. Both ASTRON and SRZM receive their funds from Z.W.O., the Netherlands Organization for the Advancement of Pure Research.

Appendix A.

RADIO LIGHT CURVES OF OH MASERS. — For all stars included in the Dwingeloo monitor program the variation of the total integrated flux density, here denoted by $F(10^{-22}\ \mathrm{W\ m^{-2}})$ is shown. The labelling of the figures refers to the numbers used in tables II and III. The light curve of U Ori (no. 8) is shown in figure 11 of section 5.2.1. Phases were calculated with the periods and phase zero points as listed in table III. Different symbols represent different cycles (squares : $n = -6$; circles : $n = -5$; triangles : $n = -4$; plusses : $n = -3$; crosses : $n = -2$; diamonds : $n = -1$; arrows : $n = 0$). For display purposes all curves are repeated; thus every observed point is shown *twice*.

The curve drawn is *not* the best fit to the observed integrated fluxes, but is based on the curves of the peak flux densities also. For the parameters describing the mean values, the amplitudes, and the shapes of the curves see table III. In the lower left corner an error bar indicates the 1-5 σ (depending on its magnitude) uncertainty for an *individual* measurement (average value).

Appendix B.

PHASE LAG AS A FUNCTION OF VELOCITY. — The phase lag, $\Delta\phi_k$, for various peaks in the spectrum is expected to be correlated with their velocities. The phase of the low velocity integrated flux is chosen as zero point and the phase difference, here denoted by DF, for every peak of a given star is plotted as a function of $1 + v/v_e$, where $v = v_{\mathrm{rad}}(\mathrm{peak}) - v_{\mathrm{rad}}(\mathrm{star})$. The drawn lines are the least squares fits, weighted with the uncertainties in the determination of each phase lag (indicated by the error bars; see table III for the values), but also with the mean signal-to-noise ratio of the peaks. The slope of the line is R_p/cP, where R_p is the radius of the shell. In the simple model adopted a negative value for the slope is « forbidden ».

References

ALLEN, D. A., HYLAND, A. R., LONGMORE, A. J., CASWELL, J. L., GOSS, W. N., HAYNES, R. F. : 1977, *Astrophys. J.* **217,** 108.
ANDERSSON, C., JOHANSSON, L. F. B., GOSS, W. N., WINNBERG, A., RIEU, NGUYEN-Q. : 1974, *Astron. Astrophys.* **30,** 475.
BAARS, J. W. M., GENZEL, R., PAULINY-TOTH, I. I., WITZEL, A. : 1977, *Astron. Astrophys.* **61,** 99.
BALL, J. A. : 1976, « Measurements with Radio-Frequency Spectrometer » in *Methods of Experimental Physics* **12C**; ed. M. L. Meeks, Chapter 4.3, p. 46 (Academic Press).
BAUD, B., HABING, H. J. : 1983, *Astron. Astrophys.* **127,** 73.
BAUD, B., HABING, H. J., MATTHEWS, H. E. : 1975, *Nature* **258,** 406.
BAUD, B., HABING, H. J., WINNBERG, A., MATTHEWS, H. E. : 1979, *Astron. Astrophys. Suppl. Ser.* **35,** 179 ; 1979, *Astron. Astrophys. Suppl. Ser.* **36,** 193 ; 1981, *Astron. Astrophys.* **95,** 156.
BENSON, J. M., MUTEL, R. L. : 1979, *Astrophys. J.* **233,** 119.
BIDELMAN, W. P. : 1980, *Publ. Warner and Swasey Obs.* (Case Western Reserve Univ.) Vol. **2,** No 6, pp. 185-273.
BLAIR, G. N., DICKINSON, D. F. : 1977, *Astrophys. J.* **215,** 552.
BLOCH, A. : 1979, *Murphy's Law and other reasons why things go wrong* (Price/Stern/Sloan Publishers, Inc., Los Angeles).
BOWERS, P. F. : 1978, *Astron. Astrophys.* **64,** 307.
BOWERS, P. F., JOHNSTON, K. J., SPENCER, J. H. : 1981, *Nature* **291,** 382.
BOWERS, P. F., KERR, F. J. : 1974, *Astron. Astrophys.* **36,** 225 ; 1977, *Astron. Astrophys.* **57,** 115 ; 1978, *Astron. J.* **83,** 487.
BOWERS, P. F., REID, M. J., JOHNSTON, K. J., SPENCER, J. H., MORAN, J. M. : 1980 *Astrophys. J.* **242,** 1088.
CAMPBELL, L. : 1955, *Studies of Long Period Variables.*
CASWELL, J. L. : 1973, « Galactic Radio Astronomy », *IAU Symp.* **60,** 423.
CASWELL, J. L., HAYNES, R. F. : 1975, *Monthly Notices Roy. Astron. Soc.* **173,** 649.
CATO, B. T., ROENNAENG, B. O., RYDBECK, O. E. J., LEWIN, P. T., YNGVESSEN, K. S., CARDIASHENOS, R. G., SHANTEY, J. F. : 1976, *Astrophys. J.* **208,** 87.
CIMERMAN, M. : 1979, *Astrophys. J. Lett.* **228,** L-79.
DICKINSON, D. F. : 1976, *Astrophys. J. Suppl.* **30,** 259.
DICKINSON, D. F., BECHIS, K. P., BARRETT, A. H. : 1973, *Astrophys. J.* **180,** 831.

DICKINSON, D. F., BLAIR, G. N. : *Bull. Am. Astron. Soc.* **8,** 348.
DICKINSON, D. F., BLAIR, G. N., DAVIS, J. H., COHEN, N. L. : 1978, *Astron. J.* **83,** 32.
DICKINSON, D. F., CHAISSON, E. J. : 1973, *Astrophys. J. Lett.* **181,** L135.
DICKINSON, D. F., KLEINMANN, S. G. : 1977, *Astrophys. J. Lett.* **214,** L135.
DICKINSON, D. F., KOLLBERG, E., YNGVESSON, S. : 1975, *Astrophys. J.* **199,** 131.
DICKINSON, D. F., SNYDER, L. E., BROWN, L. W., BUHL, D. : 1978, *Astron. J.* **83,** 36.
DYCK, H. M., LOCKWOOD, G. W., CAPPS, R. W. : 1974, *Astrophys. J.* **189,** 89.
ELITZUR, M., GOLDREICH, P., SCOVILLE, N. : 1976, *Astrophys. J.* **205,** 384.
ENGELS, D. : 1979, *Astron. Astrophys. Suppl. Ser.* **36,** 337.
ENGELS, D. : 1982, « Zur Natur von OH/IR-Objekten », Ph.D. thesis *Veröff. Astron. Inst. Bonn* **95.**
ENGELS, D., KREYSA, E., SCHULTZ, G. V., SHERWOOD, W. A. : 1983, *Astron. Astrophys.* **124,** 123.
EPCHTEIN, N., RIEU, NGUYEN-Q. : 1982, *Astron. Astrophys.* **197,** 229.
EVANS, N. J., BECKWITH, S. : 1977, *Astrophys. J.* **217,** 729.
EVANS, N. J., CRUTCHER, R. N., WILSON, W. J. : 1976, *Astrophys. J.* **206,** 440.
GEHRZ, R. D., WOOLF, N. J. : 1971, *Astrophys. J.* **165,** 285.
GILLET, F. C., MERRILL, K. M., STEIN, W. A. : 1971, *Astrophys. J.* **164,** 83.
GOLDREICH, P., KEELEY, D. A. : 1972, *Astrophys. J.* **174,** 517.
HARVEY, P. M., BECHIS, K. B., WILSON, W. J., BALL, J. A. : 1974, *Astrophys. J. Suppl.* **27,** 331.
HERBIG, G. H. : 1969, *Mém. Soc. Roy. Sic. Liège* **19,** 13.
HERMAN, J., HABING, H. J. : 1981, in *Physical Processes in Red Giants,* Eds. I. Iben and A. Renzini (Reidel) pp. 383-390.
HERMAN, J. : 1983, *The Nature of OH/IR stars,* Ph.D. thesis, RUL.
HERMAN, J., HABING, H. J. : 1984, in preparation (see HERMAN, J. : 1983, Chapter V).
HERMAN, J., BAUD, B., HABING, H. J., WINNBERG, A. : 1984a, in press (see HERMAN, J. : 1983, Chapter III).
HERMAN, J., ISAACMAN, R., SARGENT, A., HABING, H. J. : 1984b, *Astron. Astrophys.* **139,** 171.
HYLAND, A. R., BECKLIN, E. E., FROGEL, J. A., NEUGEBAUER, G. : 1972, *Astron. Astrophys.* **16,** 204.
HYLAND, A. R., BECKLIN, E. E., NEUGEBAUER, G., WALLERSTEIN, G. : 1969, *Astrophys. J.* **158,** 619.
JEWELL, P. R., ELITZUR, M., WEBBER, J. C., SNYDER, L. E. : 1979, *Astrophys. J. Suppl.* **41,** 191.
JEWELL, P. R., WEBBER, J. C., SNYDER, L. E. : 1980, *Astrophys. J. Lett.* **242,** L29.
JEWELL, P. R., WEBBER, J. C., SNYDER, L. E. : 1981, *Astrophys. J.* **249,** 118.
JOHANSSON, L. E. B., ANDERSSON, C., GOSS, W. N., WINNBERG, A. : 1977, *Astron. Astrophys. Suppl. Ser.* **28,** 199.
JOHNSTON, K. J., ROBINSON, B. J., CASWELL, J. L., BATCHELOR, R. A. : 1972, *Astrophys. Lett.* **10,** 93.
JONES, T. J., HYLAND, A. R., CASWELL, J. L., GATLEY, I. : 1982, *Astrophys. J.* **253,** 208.
JONES, T. J., HYLAND, A. R., WOOD, P. R., GATLEY, I. : 1983, *Astrophys. J.* **273,** 669.
KAIFU, N., BUHL, D., SNYDER, L. E. : 1975, *Astrophys. J.* **195,** 359.
KOLENA, J., PATAKI, L. : 1977, *Astron. J.* **82,** 150.
KUKARKIN, B. V., KHOLOPOV, P. N., EFREMOV, Yu. N., KUKARKINA, N. P., KUROCHKIN, N. F., MEDVEDEVA, G. I., PEROVA, N. B., FEDOROVICH, V. P., FROLOV, M. S. : 1969, *General catalogue of variable stars,* Moscow (+ Suppl.).
LEBOSKY, M. J., KLEINMANN, S. G., RIEKE, G. H., LOW, F. J. : 1976, *Astrophys. J. Lett.* **206,** L157.
LÉPINE, J. R. D., PAES DE BARROS, M. H., GAMMON, R. H. : 1976, *Astron. Astrophys.* **48,** 269.
LÉPINE, J. R. D., LE SQUEREN, A. M., SCALISE Jr., E. : 1978, *Astrophys. J.* **225,** 869.
LE SQUEREN, A. M., BAUDRY, A., BRILLET, J., DARCHY, B. : 1979, *Astron. Astrophys.* **72,** 39.
LOCKWOOD, G. W. : 1972, *Astrophys. J. Suppl.* **24,** 375.
LOCKWOOD, G. W., WING, R. F. : 1971, *Astrophys. J.* **169,** 63.
MENDOZA, E. E. : 1965, *Bol. Obs. Tonanzintla y Tacubaya* **4,** 51.
MERRILL, K. M., STEIN, W. A. : 1977, *Publ. Astron. Soc. Pacific* **88,** 285 ; *ibid.* **88,** 294 ; *ibid.* **88,** 874.
MORRIS, M., JURA, M. : 1983, *Astrophys. J.* **264,** 546.
MORRISON, D., SIMON, T. : 1973, *Astrophys. J.* **186,** 193.
NEUGEBAUER, G., LEIGHTON, R. B. : 1969, *Two micron sky survey,* Nasa SP-3047.
REID, M. J., MUHLEMAN, D. O., MORAN, J. M., JOHNSTON, K. J., SCHWARTZ, P. R. : 1977, *Astrophys. J.* **214,** 60.
REID, M. J., MORAN, J. M., JOHNSTON, K. J. : 1981, *Astron. J.* **86,** 897.
RIEU, NGUYEN-Q., FILLIT, R., CHEUDIN, M. : 1971, *Astron. Astrophys.* **14,** 154.
RIEU, NGUYEN-Q., LAURY-MICOULAT, C., WINNBERG, A., SCHULTZ, G. V. : 1979, *Astron. Astrophys.* **75,** 351.
ROBINSON, B. J., CASWELL, J. L., GOSS, W. N. : 1970, *Astrophys. Lett.* **7,** 79.
SCHNELLER, H. : 1965, *Sonneberg M.V.S.* Bd3, Heft 2, 86.
SCHULTZ, G. V., KREYSA, E., SHERWOOD, W. A. : 1976, *Astron. Astrophys.* **50,** 171 (see also the correction in **52,** 457).
SCHULTZ, G. V., SHERWOOD, W. A., WINNBERG, A. : 1978, *Astron. Astrophys. Lett.* **63,** L5.
SCHWARTZ, P. R., BARRETT, A. H., 1970, *Astrophys. J. Lett.* **159,** L123.
SIMON, T. : 1974, *Astron. J.* **79,** 1054.
SLOTTJE, C. : 1982, *User Note* **43,** Dwingeloo, 810508.
SNYDER, L. E., BUHL, D. : 1975, *Astrophys. J.* **197,** 329.
SPENCER, J. H., SCHWARTZ, P. R., WAAK, J. A., BOLOGNA, J. M. : 1977, *Astron. J.* **82,** 706.
STRECKER, D. W., NEY, E. P. : 1974, *Astron. J.* **79,** 794 ; 1974, *Astron. J.* **79,** 1410.
SULLIVAN, W. J. III : 1973, *Astrophys. J. Suppl.* **25,** 393.
TURNER, B. E. : 1971, *Astrophys. Lett.* **8,** 73.
WERNER, M. W., BECKWITH, S., GATLEY, I., SELLGREN, K., BERRIMAN, G. : 1980, *Astrophys. J.* **239,** 540.
WILLEMS, F., DE JONG, T. : 1982, *Astron. Astrophys.* **115,** 213.
WILSON, W. J., BARRETT, A. H. : 1972, *Astron. Astrophys.* **17,** 385.
WILSON, W. J., BARRETT, A. H., MORAN, J. N. : 1970, *Astrophys. J.* **160,** 545.
WILSON, W. J., SCHWARZ, P. R., NEUGEBAUER, G., HARVEY, P. M., BECKLIN, E. E. : 1972, *Astrophys. J.* **177,** 523.
WINNBERG, A., RIEU, NGUYEN-Q., JOHANSSON, L. E. B., GOSS, W. N. : 1975, *Astron. Astrophys.* **38,** 145.
WOOD, P. R., CAHN, J. H. : 1977, *Astrophys. J.* **211,** 499.

TABLE I.

Programstar OH	Confusion by OH	Distance (°)	Position in spectrum	Influence	References (see table 2)
11.5+0.1	11.3+0.0	0.27	In high velocity peak	Weak	30
12.3-0.1	12.3+0.1	0.30	In middle of spectrum	Peaks can be removed	23
17.4-0.3	17.0-0.1	0.45	In high velocity part	HV peak has large scatter	58
18.3+0.4	18.3+0.1	0.30	All spectrum	Very strong	18
20.2-0.1	20.4-0.3	0.28	In middle of spectrum	Peaks can be removed	19,40
20.7+0.1	20.6+0.3	0.22	Just outside spectrum (LV)	Baseline poor	35
21.5+0.5	21.9+0.4	0.41	In low velocity part	Weak	35
25.1-0.3	24.7-0.1	0.45	In low velocity part	Large scatter	8,19,40
27.3+0.2	27.2+0.2	0.10	Same source?	None?	1,41
	27.2+0.2	0.10	Just outside spectrum (HV)	Baseline mildly afflicted	23,35
30.1-0.7	30.1-0.2	0.50	Weak	Baseline uncertain	8,13,20,28,47
30.1-0.2	30.1-0.7	0.50	Outside spectrum (LV)	Baseline bad	8,12,13,20,28
30.7+0.4	30.9+0.2	0.28	In middle of spectrum	Peaks can be removed	24
	31.0+0.0	0.50	Outside spectrum (LV)	Baseline very bad	1,46
31.0-0.2	30.9+0.2	0.51	Outside spectrum	Baseline very bad	24
	31.0+0.0	0.20	Outside spectrum		1,46
	31.2-0.2	0.20	?		
	31.5-0.1	0.51	Outside spectrum		19,40
31.0+0.0	30.7+0.4	0.50	Outside spectrum (HV)	Baseline very bad	18,19,24,40
	30.9+0.2	0.37	Outside spectrum (LV)		24
	31.0-0.2	0.20	Outside spectrum (HV)		8,19,24,40
	31.5-0.1	0.50	Outside spectrum (LV)		19,40
32.0-0.5	31.7-0.8	0.42	In middle of spectrum	Peak can be removed	18,19,40
35.6-0.3	35.3-0.7	0.50	Weak	None	

TABLE IIa

No.	Name	IRC AFGL	P_R P_o (days)	$\pm\Delta P$	Δm_R Δm_V (mag)	v_* (LSR) $\pm$ (km s^{-1})	Range $\pm$ (km s^{-1})	Julian Days (+244 0000)	#	IR VLA	References
1	R Aql	+10406	279.6	2.3	0.87	+ 47.17 0.03	16.18 0.06	3029-5265	84	A,C	1,3,10,11,17,23
		2324	285.6		6.3					a	33,36,43,53,58
2	RR Aql	+00458	403.8	2.2	0.71	+ 27.77 0.04	15.02 0.11	3689-5271	77	A	1,3,5,17,22,27
		2479	394.33		6.7					a	33,34,36,54,58
3	SY Aql	+10450	349.3	7.9	0.62	- 47.96 0.04	11.30 0.12	3702-5266	110		2,4,27,36,46,
			355.74		7.1						58
4	VY CMa	-30087	988.8:	34.3	0.18	+ 23.67 0.04	74.35 0.04	4317-5267	146	A	3,14,17,22,38,39
		1111			0.9					a,b,c	48,49,52,55
5	PZ Cas	+60417	707.3:	52.3	0.29	- 37.42 0.05	60.33 0.19	4317-5267	62		2,7,14,29,54,
			900:		2.9						58
+ 6	NML Cyg	+40448	1109.6:	35.7	0.31	- 1.97 0.01	53.70 0.04	4074-5269	177	A	3,11,14,17,22,26
	=OH80.8-1.9	2650	1280:							a	34,37,49,51,53
7	Z Cyg	+50314	270.3	2.1	0.70	-148.25 0.04	6.79 0.08	3690-5268	117		2,4,27,36,46,
			263.85		7.1						58
8	U Ori	+20127	406.3	10.1	(0.94)	- 44.22 0.04	8.65 0.11	3694-5269	91	A	6,10,14,15,27,36
			372.45		7.3					a	43,44,45,54,58
9	WX Psc	+10011	632.0	17.6	1.16	+ 8.96 0.03	38.37 0.05	3029-5268	71	A	1,2,13,16,17,22
		157	660(IR)							a,b,c	33,49,51,53,55
10	WX Ser	+20281	443.0	7.9	0.58	+ 5.95 0.04	17.72 0.09	3688-5266	110	G	1,2,3,14,17,26,27
			425.1		4.					a	43,45,48,51,53,58
11	IK Tau	+10050	455.6	5.7	1.33	+ 33.66 0.04	36.01 0.05	3694-5268	85		1,3,5,13,16,17,42
	=NML Tau	529	460		4.6						49,51,53,58
12	RS Vir	+00243	363.8	9.	0.48	- 14.91 0.03	11.12 0.05	3688-5266	132	G	4,9,27,36,44,46,
			352.80		7.4						58

TABLE IIb

No	Name	P_R / P_{IR} (days)	±ΔP	Δm_R (mag)	$v_\star$(LSR) ± (km s^{-1})	Range ± (km s^{-1})	Julian Days (+244 0000)	#	IR / VLA	References	Remarks
	OH———										
13	359.4-1.3	(930)	115	0.13	-219.58 0.07	35.76 0.12	4318-5269	35		30	Not variable
14	0.3-0.2	(243)	15	0.16	-340.88 0.07	33.63 0.10	3029-5270	48	c	31	Not variable
15	1.5-0.0	(141)	8	0.21	-127.63 0.08	28.72 0.11	4318-5270	32	c	30	Not variable
+ 16	11.5+0.1	691:	40	0.23	+ 41.79 0.11	61.33 0.13	4318-5271	34		30	Variable?
+ 17	12.3-0.2	544	15	0.56	+ 36.60 0.12	30.21 0.16	4318-5269	29	F?	23	
+ 18	12.8-1.9	812	56	0.56	+ 10.44 0.06	47.78 0.14	4318-5270	27	E,G	35	
+ 19	12.8+0.9	1488	81	0.34	+ 26.91 0.07	24.71 0.13	4318-5269	32		23	
+ 20	13.1+5.0	707	40	0.53	- 67.73 0.07	33.89 0.19	4318-5269	27		35	
+ 21	15.7+0.8	(453)	42	0.13	- 0.62 0.04	31.96 0.06	4318-5269	30		23	Not variable
+ 22	16.1-0.3	1012	50	0.55	+ 21.13 0.05	46.70 0.06	4318-5271	33		23	
+ 23	17.4-0.3	1219	40	0.59	+ 29.13 0.08	36.21 0.13	4318-5269	31		23	
+ 24	17.7-2.0	890:	61	0.16	+ 61.19 0.04	28.33 0.03	3688-5266	47	G a	23	Variable?
+ 25	18.3+0.4	845:	56	0.27	+ 47.93 0.05	32.66 0.08	4318-5269	31	B,F	8,25	Variable?
+ 26	18.5+1.4	1125:	86	0.19	+176.17 0.06	24.25 0.14	3688-5268	102	d	23,35	Variable?
+ 27	18.8+0.3	923	20	0.26	+ 12.75 0.05	31.87 0.08	4318-5269	34		1,40	
+ 28	20.2-0.1	857 680	44 40	0.67	+ 26.60 0.07	35.44 0.13	4318-5271	35	B,C,G	18,19,40	
+ 29	20.7+0.1	1130	40	0.99	+136.55 0.04	38.97 0.05	3029-5271	60	B,G d	13,18,19,23,40	
+ 30	21.5+0.5	1975:	60	1.09	+115.77 0.04	40.07 0.06	4318-5271	59	D,G d	8,20,28	
+ 31	25.1-0.3	226:	11	0.21	+142.88 0.08	26.83 0.08	4318-5269	35	F? a,d	19,40	Variable?
+ 32	26.2-0.6	1181 1330	13 50	1.05	+ 72.04 0.07	46.78 0.05	3689-5276	53	B,C,G	18,19,23,40	
+ 33	26.4-1.9	652 540	26 20	0.44	+ 27.65 0.05	26.72 0.10	4318-5270	33	B,C,E,G	18,19,23,40	
+ 34	26.5+0.6 AFGL 2205	1566 1630	16 100	1.13	+ 26.86 0.03	30.69 0.02	3029-5266	70	C,D,E a,b,c,d	13,18,20,21,28 32,40,50,57	
+ 35	27.3+0.2	939	35	0.59	+ 50.42 0.05	28.21 0.10	4318-5269	23		1,41	
+ 36	28.5-0.0	559	16	0.77	+107.65 0.06	28.79 0.07	4318-5270	26	B,G d	19,40	
+ 37	28.7-0.6	627 640	17 10	0.83	+ 46.45 0.04	37.31 0.09	4318-5270	35	B,C,G	18,19,23,40	
+ 38	30.1-0.7	2060: 1730	130 200	0.40	+ 99.26 0.04	43.57 0.05	3689-5265	55	C,G d	8,12,13,20,28	
+ 39	30.1-0.2	853 970	21 40	0.81	+ 50.53 0.05	37.75 0.08	4318-5270	31	C,D,G	8,13,20,28,47	
+ 40	30.7+0.4	1039 1140	27 30	0.57	+ 66.59 0.06	37.03 0.08	3029-5265	52	B,C,G	18,19,24,40	
+ 41	31.0-0.2	(1126)	100	0.13	+125.98 0.06	31.09 0.09	4318-5266	33	B,F,G d	8,19,40,46	Not variable
+ 42	31.0+0.0 W43A	400:	8	0.21	+ 35.10 0.03	17.83 0.05	3689-5269	112		1,46	Variable?
+ 43	32.0-0.5	1540	83	0.88	+ 76.04 0.06	43.70 0.08	4318-5270	36	G d	8,19	

TABLE IIb *(continued)*

No	Name	P_R / P_{IR} (days)	±ΔP	Δm_R (mag)	v_*(LSR) ± (km s^{-1})	Range ± (km s^{-1})	Julian Days (+244 0000)	#	IR / VLA	References	Remarks
	OH ———										
+ 44	32.8-0.3	1536	10	1.24	+ 60.75 0.04	35.32 0.06	3029-5265	77	B,C,D,G	13,18,20,28,40,47	
		1750	130						a,d		
+ 45	35.6-0.3	840	40	0.78	+ 78.00 0.05	29.59 0.07	3029-5269	36		1,41	
46	36.9+1.3	409	5	0.56	- 12.22 0.03	17.20 0.05	3688-5271	86		35	
+ 47	37.1-0.8	(737)	61	0.13	+ 88.48 0.05	29.72 0.07	3029-5269	37		19,23,35,40	Not variable
									d		
+ 48	39.7+1.5	1424	16	0.82	+ 20.00 0.03	35.71 0.05	3689-5265	52	G	23,32,35,57	
	AFGL 2290								a		
+ 49	39.9-0.0	823	45	0.80	+148.84 0.04	31.97 0.08	4318-5270	39	C,G	19,35,40	
		770	20						a		
+ 50	42.3-0.1	1945	83	0.36	+ 59.19 0.04	35.29 0.06	3689-5266	54	B,C,G	19,23,35,40	
		1650	150								
+ 51	44.8-2.3	552	5	0.77	- 71.56 0.03	34.26 0.07	4325-5269	28		23,35	
	AFGL 2374										
+ 52	45.5+0.1	760	31	0.92	+ 34.97 0.08	36.80 0.14	4325-5269	31	C,D	8,13,18,20,28,41	
	AFGL 2345	720	20								
+ 53	51.8-0.2	(1162)	71	0.16	+ 2.01 0.05	41.22 0.09	4318-5271	31		23,35	Not variable
+ 54	53.6-0.2	(838)	110	0.12	+ 10.47 0.04	29.23 0.08	4324-5270	28		23,35	Not variable
+ 55	75.3-1.8	1603:	54	1.08	- 3.48 0.05	26.60 0.09	4323-5272	36		23,35	
+ 56	77.9+0.2	(1339)	113	0.19	- 39.08 0.05	24.64 0.07	4317-5269	35		1,39	Not variable
+ 57	83.4-0.9	1153	40	1.28	- 38.54 0.02	38.77 0.04	4318-5267	128		23,35	
+ 58	104.9+2.4	1215:	54	0.66	- 25.62 0.02	32.38 0.03	4318-5268	82		23,35,46	
	AFGL 2885								a		
+ 59	127.9-0.0	1994:	130	1.47	- 54.97 0.02	24.50 0.02	3030-5268	86		23,24,35,57	
	AFGL 230								a		
+ 60	138.0+7.2	1352:	136	0.81	- 37.72 0.03	21.28 0.05	4318-5268	79		23,35	
									a		

V.L.A. Observations

a. Bowers *et al.* (1981)
b. Reid *et al.* (1981)
c. Baud
d. Herman et al. (1984a)

I.R. observations

A. Harvey *et al.* (1974)
B. Jones *et al.* (1982)
C. Engels (1982)
D. Werner *et al.* (1980)
E. Willems, de Jong (1982)
F. Epchtein, Rieu (1982)
G. Herman et al. (1984b)

References to Tables I, II and III.

1. Wilson and Barrett (1972)
2. Dickinson (1976)
3. Snyder and Buhl (1975)
4. Dickinson *et al.* (1975)
5. Dickinson *et al.* (1973)
6. Wilson *et al.* (1972)
7. Dickinson and Chaisson (1973)
8. Rieu *et al.* (1971)
9. Johnston *et al.* (1972)
10. Lépine *et al.* (1976)
11. Schwartz and Barrett (1970)
12. Cato *et al.* (1976)
13. Dickinson and Blair (1977)
14. Kaifu *et al.* (1975)
15. Spencer *et al.* (1977)
16. Dyck and Lockwood (1974)
17. Hyland *et al.* (1972)
18. Schultz *et al.* (1976)
19. Johansson *et al.* (1977)
20. Evans *et al.* (1976)
21. Andersson *et al.* (1974)
22. Harvey *et al.* (1974): A
23. Bowers (1978)
24. Bowers and Kerr (1974)
25. Caswell and Haynes (1975)
26. Caswell (1973)
27. Rieu *et al.* (1979)
28. Evans and Beckwith (1977)
29. Bowers and Kerr (1978)
30. Baud *et al.* (1979a)
31. Baud *et al.* (1975)
32. Allen *et al.* (1977)
33. Blair and Dickinson (1977)
34. Dickinson and Kleinman (1977)
35. Baud *et al.* (1979b)
36. Lockwood (1972)
37. Wilson *et al.* (1970)
38. Robinson *et al.* (1970)
39. Sullivan III (1973)
40. Winnberg *et al.* (1975)
41. Turner (1971)
42. Mendozo (1967)
43. Lockwood and Wing (1971)
44. Gillet *et al.* (1971)
45. Gehrz and Woolf (1971)
46. Dickinson *et al.* (1978a)
47. Dickinson *et al.* (1978b)
48. Merrill and Stein (1977a)
49. Merrill and Stein (1977b)
50. Merrill and Stein (1977c)
51. Strecker and Ney (1974)
52. Hyland *et al.* (1969)
53. Morrison and Simon (1973)
54. Simon (1974)
55. Lépine *et al.* (1978)
56. Le Squeren *et al.* (1979)
57. Lebofsky *et al.* (1976)
58. Kukarkin *et al.* (1969)

TABLE III.

	Name	P_R / JD_o (Days)	f_R	m_l	Log $\bar{S}_{LV}$ / Log $\bar{S}_{HV}$ (Log 10^{-22} Wm^{-2})	m.e. (1σ)	$\Delta\phi$ (HV-LV) (10^{-4})	±	$v_k - v_*$ (km s^{-1})	fw_k (km s^{-1})	Log $\bar{S}_k$ (Log Jy)	m.e.$_k$ (1σ)	$\Delta\phi_k$ (10^{-4})	±
1	R Aql	279.6	0.53	0.174	0.828	.035	123	69	- 6.16	1.88	0.601	.052	130	68
		5177.8			1.652	.005			- 3.72	0.96	0.605	.052	- 383	43
									+ 6.88	0.95	1.883	.003	404	74
2	RR Aql	403.8	0.42	0.142	0.695	.041	47	28	- 6.59	0.71	0.047	.175	- 262	60
		4986.0			0.818	.031			- 4.92	1.35	0.696	.037	19	20
									+ 4.93	1.13	0.881	.025	41	26
									+ 6.37	1.05	0.427	.070	41	28
3	SY Aql	349.3	0.45	0.123	0.187	.065	- 269	200	- 4.87	0.85	-0.127	.147	- 409	224
		5181.9			0.233	.058			- 3.78	0.80	-0.054	.123	58	139
									- 2.54	0.98	0.139	.078	- 298	181
									+ 1.85	0.74	-0.168	.163	2373	129
									+ 3.20	1.60	0.092	.087	- 326	236
									+ 4.09	1.40	0.032	.100	- 79	165
									+ 5.06	0.61	-0.179	.167	372	354
4	VY CMa	998.9:	0.42	0.036	2.880	.003	- 185	55	-36.00	0.87	1.713	.015	907	83
		5078.9			2.862	.003			-34.28	1.57	2.336	.004	964	107
									-31.58		2.264	.005	317	66
									-30.17		2.364	.004	488	83
									-28.16		2.111	.006	485	81
									-26.97		2.000	.008	8	56
									-25.25		1.567	.022	32	62
									-13.75	0.75	1.161	.055	909	113
									+11.84	1.61	1.474	.027	298	86
									+13.58	0.91	1.659	.017	- 38	75
									+14.78		1.707	.016	-1363	74
									+17.14		1.744	.014	- 85	71
									+18.75		1.788	.013	-1391	109
									+20.61		1.787	.013	4980	165
									+22.16		1.871	.011	- 582	85
									+23.75		1.974	.009	- 157	52
									+26.07		1.956	.009	210	66
									+28.48		2.041	.007	354	49
									+29.68		1.997	.008	385	53
									+31.03		1.813	.012	315	69
5	PZ Cas	707.3	0.34	0.059	0.836	.051	275	168	-28.94		-0.005	.168	3051	423
		5019.0			0.864	.048			-27.09		0.651	.036	- 94	106
									-25.85		0.392	.065	395	216
									-24.62		0.172	.109	482	195
									+ 9.56		-0.096	.213	161	212
									+24.72		0.480	.053	- 68	106
									+25.93		0.464	.055	439	105
									+28.32		0.073	.138	177	134
6	NML Cyg	1109.6	0.38	0.062	3.030	.002	- 243	49	-23.05		2.542	.003	75	38
		4904.2			2.494	.006			-21.70	1.22	2.695	.002	82	39
									-19.16		2.166	.006	75	39
									-18.38		2.155	.006	48	28
									-16.50		2.335	.004	63	37
									-15.13		1.809	.014	- 216	54
									+10.62	1.59	1.488	.029	34	29
									+12.17	1.35	1.473	.030	- 14	11
									+18.74	1.59	1.432	.033	- 170	46
									+22.33		1.959	.010	62	38
									+23.80		2.139	.007	77	39
7	Z Cyg	270.3	0.43	0.140	0.365	.044	47	98	- 2.11	0.90	0.609	.034	- 91	34
		5194.1			-0.127	.077			+ 1.78	0.96	-0.002	.145	- 91	54
									+ 2.91	0.65	-0.287	.314	864	152
8	U Ori	406.3	0.39	0.188	0.130	.090	506	114	- 4.37		-0.172	.237	-3309	82
		4959.8			0.401	.048			- 2.92	1.11	0.306	.073	131	43
									+ 2.63	0.84	0.669	.031	553	110
									+ 3.78		-0.151	.224	1398	244
9	WX Psc	632.0	0.31	0.232	1.353	.017	311	5	-18.28	0.96	1.556	.006	20	5
		4955.7			1.292	.019			+18.21	0.96	1.486	.007	351	7
10	WX Ser	443.0	0.42	0.116	0.441	.050	- 217	76	- 8.19		-0.230	.212	1234	112
		5212.3			0.275	.073			- 6.93	1.85	0.338	.054	11	57

TABLE III *(continued)*.

	Name	P_R JD$_o$ (Days)	f_R	m_l	Log $\bar{S}_{LV}$ / Log $\bar{S}_{HV}$ (Log 10^{-22} Wm^{-2})	m.e. (1σ)	$\Delta\phi$(HV-LV) (10^{-4})	±	$v_k - v_*$ (km s^{-1})	fw_k (km s^{-1})	Log $\bar{S}_k$ (Log Jy)	m.e.$_k$ (1σ)	$\Delta\phi_k$ (10^{-4})	±
									- 6.38	1.64	0.319	.056	246	93
									- 5.51		0.219	.071	- 81	42
									+ 5.04	0.96	-0.235	.215	4217	87
									+ 6.54	0.70	0.087	.096	- 135	40
									+ 7.71	0.88	0.396	.047	- 342	98
11	IK Tau	455.6	0.48	0.267	0.595	.063	54	24	-17.57	0.57	-0.004	.153	321	24
		5078.5			0.658	.054			-16.25	0.99	0.627	.035	136	16
									-14.57	0.96	-0.134	.214	- 31	27
									-13.42	0.83	-0.187	.248	10	67
									+13.33	0.86	0.323	.070	92	26
									+14.53	1.41	0.074	.122	89	17
									+15.29	0.94	0.075	.121	- 90	54
									+17.03	0.97	0.513	.045	174	24
12	RS Vir	363.8	0.42	0.095	0.489	.034	155	78	- 4.80	0.74	-0.289	.239	719	142
		5088.7			0.616	.026			- 3.52		0.240	.065	- 144	51
									- 2.62		0.276	.060	366	56
									- 1.57	0.87	0.216	.069	- 232	47
									- 0.38	0.64	-0.172	.175	- 77	123
									+ 4.66	0.98	0.817	.017	70	50
13	359.4-1.3	(933)	(0.37)	0.027	1.018	.034			-16.88		0.319	.103		
		(4907.6)			0.918	.043			-15.16	1.66	0.775	.036		
									-13.73	0.86	0.575	.057		
									+16.62	1.16	0.915	.026		
14	0.3-0.2	(243)	(0.41)	0.033	0.911	.069			-15.24	1.17	0.713	.067		
		(5116.0)			0.966	.061			-13.56	1.38	0.484	.115		
									-12.49	1.03	0.380	.148		
									+13.40	1.65	0.582	.091		
									+14.23	1.31	0.619	.083		
									+15.41	1.17	0.593	.089		
									+16.33		0.426	.132		
15	1.5-0.0	(141)	(0.36)	0.042	0.573	.082			-13.63	0.95	0.677	.043		
		(5107.9)			0.720	.058			-11.63	0.81	0.050	.191		
									+13.44	0.84	0.898	.026		
16	11.5+0.1	691.4:	0.34	0.046	1.285	.031	1522	318	-28.33	1.16	0.342	.125	-1920	289
		5016.0			2.059	.005			-25.88		0.473	.092	- 9	211
									-22.78		0.575	.072	100	75
									-21.24	1.50	0.761	.047	40	40
									+14.64		0.906	.034	- 127	70
									+17.86		0.986	.028	- 81	58
									+22.38	3.78	1.495	.009	24	295
									+25.70		1.121	.021	104	278
									+28.01		1.252	.015	56	49
17	12.3-0.2	543.8	0.50	0.113	0.881	.040	- 331	88	-13.28	1.48	0.734	.036	- 570	44
		5133.4			0.876	.040			-11.48	1.04	0.232	.118	-1082	167
									+13.68	1.03	0.861	.027	- 821	121
18	12.8-1.9	812.3	0.43	0.112	1.413	.012	136	38	-23.13		0.431	.060	57	39
		4912.8			1.240	.018			-22.19	0.68	0.809	.025	- 125	33
									-20.31	1.30	0.468	.055	869	29
									-18.45		0.955	.018	592	35
									-17.25	1.52	1.152	.012	- 133	32
									+15.58		0.377	.069	822	39
									+16.58		0.396	.066	511	64
									+18.16		0.502	.051	738	54
									+20.39		0.789	.027	995	57
									+21.49	3.07	0.830	.024	167	35
19	12.8+0.9	1487.8	0.35	0.067	0.942	.025	- 602	250	-11.27	0.84	0.689	.032	2756	214
		4247.3			0.985	.022			- 9.29	1.77	0.614	.038	1767	364
									- 7.54		0.240	.089	273	317
									- 6.61		0.232	.091	-1840	428
									- 5.50	0.99	0.069	.135	156	220
									+ 6.39		0.049	.142	305	410
									+ 8.04		0.530	.046	390	223
									+ 9.46		0.486	.050	127	202
									+10.94	1.44	0.657	.034	- 40	256
20	13.1+5.0	707.5	0.45	0.106	1.134	.017	926	55	-14.65	1.74	1.135	.010	145	47
		4872.6			0.757	.040			+13.61		0.391	.057	864	64
									+15.20	1.05	0.746	.025	971	42
21	15.7+0.8	(453)	(0.38)	0.027	1.626	.010			-14.56	0.99	1.646	.009		
		(4896.8)			1.464	.014			-13.39		1.228	.015		
									- 8.68	2.10	0.485	.085		
									- 7.51	2.06	0.491	.083		
									+11.28	1.24	0.707	.050		
									+14.20	1.62	1.341	.012		

TABLE III *(continued)*.

	Name	P_R (Days)	f_R	m_l	Log $\bar{S}_{LV}$ / Log $\bar{S}_{HV}$ (Log 10^{-22} Wm^{-2})	m.e. (1σ)	$\Delta\phi$(HV-LV) (10^{-4})	±	$v_k - v_*$ (km s^{-1})	fw_k (km s^{-1})	Log $\bar{S}_k$ (Log Jy)	$m.e._k$ (1σ)	$\Delta\phi_k$ (10^{-4})	±
22	16.1-0.3	1011.7	0.46	0.111	1.579	.013	156	53	-22.37	1.03	1.102	.020	14	11
		5055.2			1.579	.013			-20.39		0.988	.026	- 47	35
									-18.31		0.997	.026	- 102	33
									-16.26		0.703	.050	181	39
									-11.52		0.465	.087	30	38
									+ 9.41		0.409	.100	803	45
									+11.25		0.479	.085	515	64
									+13.92		0.617	.061	476	64
									+17.09		0.810	.039	403	64
									+20.31		0.964	.028	67	31
									+22.02	1.04	1.337	.012	68	21
23	17.4-0.3	1219.2	0.48	0.118	0.944	.031	350	239	-16.63	1.18	0.873	.022	- 69	229
		4449.8			0.677	.058			-15.05		0.350	.072	- 989	340
									+14.56	1.51	0.012	.163	-1105	246
									+17.36	0.93	0.741	.029	- 55	229
24	17.7-2.0	890.1:	0.48	0.032	2.031	.005	- 300	133	-12.19	1.82	1.915	.004	287	74
		5093.1			2.140	.004			-10.75		1.606	.008	601	190
									- 8.54		0.705	.062	1189	141
									+ 7.20		0.665	.069	3635	101
									+ 8.16	1.80	0.848	.045	- 382	158
									+ 9.83		1.040	.029	- 233	180
									+11.57		2.007	.003	2	136
									+13.20		1.873	.004	101	88
25	18.3+0.4	845.1:	0.44	0.053	0.980	.037	2900	315	-15.23	1.35	0.893	.028	2180	350
		5010.2			1.066	.030			- 9.34	1.51	0.145	.163	4587	445
									+ 9.99	1.38	-0.000	.239	-1872	520
									+12.22		0.434	.081	3048	208
									+14.03		0.508	.068	5452	205
									+15.55	1.11	0.927	.026	2670	367
26	18.5+1.4	1124.9:	0.47	0.039	1.017	.021	95	161	-10.10	1.74	0.935	.018	445	249
		5124.6			1.047	.020			- 7.40	1.02	0.241	.091	- 209	78
									- 6.38	0.79	0.071	.138	95	209
									+ 6.42	1.00	0.261	.087	305	179
									+ 7.59		0.342	.072	-1716	414
									+ 8.88		0.620	.038	- 387	125
									+ 9.90		0.741	.029	552	180
									+11.02		0.740	.029	204	172
27	18.8+0.4	923.3	0.36	0.052	1.536	.011	- 66	38	-14.65	1.65	1.541	.007	362	156
		5041.3			1.331	.018			-12.01		0.538	.070	- 496	87
									+ 9.37	1.26	0.349	.109	619	300
									+14.74	1.18	1.375	.010	223	33
28	20.2-0.1	856.6	0.44	0.133	0.901	.037	- 132	59	-15.99	1.15	0.851	.025	632	102
		5182.2			0.920	.035			-14.32		0.313	.086	- 195	70
									-12.63	0.81	-0.034	.200	2956	239
									+13.48		0.113	.138	1709	55
									+14.87		0.350	.078	- 920	141
									+16.58	1.52	0.793	.028	755	98
29	20.7+0.1	1129.5	0.42	0.199	1.140	.022	212	24	-18.40	0.97	1.147	.012	- 626	80
		5028.3			1.023	.029			-16.19	1.28	0.400	.069	- 197	18
									-15.37	1.43	0.371	.074	124	23
									+14.19		0.357	.077	566	32
									+14.76		0.351	.078	292	23
									+16.17		0.587	.045	93	100
									+18.02	1.66	0.729	.032	221	26
									+19.13		0.376	.073	438	32
30	21.5+0.5	1975.2	0.43	0.218	1.500	.013	76	17	-18.88		1.224	.014	- 105	43
		3950.5			1.399	.017			-17.86		1.243	.013	- 18	16
									-16.32		0.816	.035	205	34
									-12.40	1.99	0.514	.071	289	78
									+15.37	1.07	0.441	.085	857	56
									+16.34	1.01	0.516	.071	1021	75
									+18.65	1.10	1.393	.010	559	42
31	25.1-0.3	226.3:	0.53	0.043	0.854	.041	98	184	-12.46	0.89	0.916	.025	651	318
		5074.8			0.771	.050			-11.19		0.259	.114	(4941)	445
									+10.45	1.09	0.077	.178	557	489
									+12.35	1.00	0.806	.032	994	173
32	26.2-0.6	1180.6	0.31	0.210	1.389	.035	10	7	-22.04	0.94	1.246	.025	48	40
		4556.5			1.210	.053			-20.80	1.09	1.116	.034	43	42
									-19.71		0.823	.068	150	64
									+21.00		0.957	.050	45	40
									+22.16		0.885	.058	49	41
33	26.4-1.9	652.2	0.42	0.088	0.937	.027	- 64	147	-11.82	1.07	1.049	.014	- 100	141
		4659.2			1.170	.016			-10.09		0.231	.094	2851	136
									+ 9.46	0.74	0.128	.120	2721	189
									+10.48	0.80	0.314	.077	87	247
									+12.55	1.35	1.232	.009	17	156

TABLE III *(continued)*.

	Name	P_R JD$_o$ (Days)	f_R	m_l	Log $\bar{S}_{LV}$ m.e. Log $\bar{S}_{HV}$ (1σ) (Log 10^{-22} Wm^{-2})	$\Delta\phi$(HV-LV) ± (10^{-4})	v_k-v_* (km s^{-1})	fw_k (km s^{-1})	Log $\bar{S}_k$ (Log Jy)	m.e.$_k$ (1σ)	$\Delta\phi_k$ (10^{-4})	±
34	26.5+0.6	1566.0	0.40	0.227	2.365 .004	188 24	-14.70		1.914	.006	36	11
		4824.8			2.611 .002		-13.70	1.18	2.266	.003	- 65	14
							-12.41		1.814	.008	- 93	19
							-10.87		1.403	.020	- 38	21
							- 9.13		1.349	.022	- 107	16
							+ 7.25		1.048	.045	625	31
							+ 8.41		1.336	.023	- 86	26
							+ 9.79		1.526	.015	100	17
							+10.86		1.664	.011	140	27
							+11.80		1.758	.009	113	24
							+12.83		1.893	.007	266	41
							+14.44	1.15	2.613	.001	99	31
35	27.3+0.2	939.3	0.42	0.118	1.456 .012	- 27 84	-12.32	1.36	1.484	.008	540	159
		4837.8			1.198 .022		- 9.31		0.455	.083	1097	168
							+ 8.48		0.363	.103	923	163
							+11.58		0.761	.041	98	187
							+12.79	1.04	0.987	.024	570	141
36	28.5-0.0	559.2	0.46	0.153	1.094 .034	120 51	-13.34	1.07	1.038	.026	- 144	54
		4968.9			1.141 .030		-11.61		0.765	.048	- 167	57
							- 8.82		0.204	.183	25	104
							+ 9.56		0.222	.175	- 686	116
							+11.41		0.619	.067	- 138	24
							+13.40	1.47	1.017	.027	- 141	17
37	28.7-0.6	627.2	0.44	0.166	1.111 .019	- 13 42	-17.16	1.36	1.092	.012	- 122	12
		4767.3			0.974 .026		-12.07	1.82	-0.039	.164	357	74
							+16.69		0.690	.029	92	45
							+17.79		0.906	.018	46	41
38	30.1-0.7	2064.4	0.34	0.081	1.962 .014	122 27	-20.61	1.26	1.791	.011	- 334	30
		5330.5			2.028 .012		-17.28		1.076	.057	- 301	34
							-15.96		1.160	.047	- 386	33
							-14.14		0.996	.068	- 104	29
							+ 6.37		0.576	.189	- 375	34
							+ 8.28		0.813	.105	- 129	46
							+ 9.78		0.806	.107	- 95	35
							+11.86		0.832	.100	- 324	29
							+15.18		0.962	.074	13	35
							+17.20		1.059	.059	- 397	45
							+20.03	1.76	1.805	.011	- 202	30
39	30.1-0.2	852.5	0.38	0.163	1.257 .028	- 21 26	-17.42	1.89	1.090	.024	- 46	19
		5334.6			1.306 .025		-16.18		0.843	.042	56	29
							-14.47		0.382	.124	326	46
							-13.06	1.49	0.389	.122	- 187	44
							+15.08		0.663	.064	- 26	21
							+17.55	1.91	1.064	.025	84	26
40	30.7+0.4	1038.6	0.41	0.115	1.105 .055	2088 135	-17.55	0.88	0.973	.022	125	33
		4987.4			1.013 .068		-16.34		0.593	.053	321	101
							-15.08		0.389	.085	143	65
							-13.61		0.200	.134	- 101	155
							-12.81		0.084	.179	-2058	140
							-11.95		0.118	.164	-1398	77
							-11.05		0.230	.125	5035	112
							- 9.78	0.85	0.551	.058	-1786	118
							+13.42	1.17	0.072	.185	328	98
							+16.33		0.496	.066	812	104
							+17.52	1.11	0.724	.039	897	89
41	31.0-0.2	(1126.)	(0.41)	0.026	0.996 .043		-14.35	1.35	0.727	.050		
		(4855.2)			1.096 .034		-13.22		0.590	.069		
							-11.32		0.420	.104		
							-10.23	1.20	0.455	.095		
							+11.96		0.662	.059		
							+13.04		0.733	.050		
							+14.52		0.895	.034		
42	31.0+0.0	399.8:	0.50	0.041	1.004 .028	1280 62	- 8.23		0.923	.028	589	452
		4988.9			1.574 .008		- 7.40	1.33	1.162	.016	1246	67
							+ 3.51		0.639	.054	301	355
							+ 5.40	1.00	1.707	.005	1806	327
							+ 7.51	0.98	0.702	.047	1044	75
43	32.0-0.5	1540.2	0.45	0.175	1.314 .018	302 34	-20.56	1.02	1.014	.019	- 82	27
		5027.2			1.079 .030		-19.33		0.845	.028	- 380	44
							-18.23		0.762	.034	- 344	63
							-16.87		0.588	.051	- 14	50
							-13.23		0.279	.105	- 88	61
							+ 8.54		0.216	.122	-1847	53
							+15.97		0.184	.132	895	72
							+18.15		0.404	.078	146	26
							+20.07	1.62	0.775	.033	295	23
44	32.8-0.3	1536.3	0.37	0.248	1.841 .006	665 8	-16.43		1.319	.011	- 71	6
		4542.3			1.509 .012		-15.04		1.469	.008	- 62	6

TABLE III *(continued)*.

	Name	P_R / JD_o (Days)	f_R	m_l	Log $\bar{S}_{LV}$ / Log $\bar{S}_{HV}$ (Log 10^{-22} Wm^{-2})	m.e. (1σ)	$\Delta\phi$(HV-LV) (10^{-4})	±	v_k-v_* (km s^{-1})	fw_k (km s^{-1})	Log $\bar{S}_k$ (Log Jy)	$m.e._k$ (1σ)	$\Delta\phi_k$ (10^{-4})	±
									-13.13		1.166	.015	- 110	5
									-10.95		0.811	.034	19	8
									-10.01		0.802	.035	- 324	18
									- 9.08		0.855	.031	- 198	4
									- 7.54		0.651	.049	- 348	13
									+10.29		0.556	.061	786	16
									+11.43		0.689	.045	432	7
									+13.54		1.024	.021	459	6
									+15.51		1.220	.013	408	5
45	35.6-0.3	839.8	0.44	0.156	1.391	.016	282	245	-13.66	1.42	1.317	.013	- 44	156
		5178.9			1.217	.024			-12.49		0.963	.028	1131	282
									- 9.78	1.76	0.564	.071	199	88
									+ 9.68		0.409	.103	274	331
									+11.21		0.558	.072	422	76
									+13.60	1.07	1.211	.016	503	173
46	36.9+1.3	409.0	0.38	0.113	0.462	.066	47	30	- 7.62	0.94	0.642	.038	- 20	21
		5050.6			0.453	.068			- 6.39		-0.008	.175	- 117	83
									+ 6.67		0.125	.126	-1371	106
									+ 7.90	0.82	0.643	.037	- 40	25
47	37.1-0.8	(737)	(0.45)	0.027	1.266	.017			-13.30		0.955	.022		
		(4988.9)			1.291	.016			-11.62	1.12	1.095	.016		
									- 8.89	1.68	0.362	.088		
									- 7.67	0.91	0.235	.119		
									+ 9.70	1.66	0.388	.083		
									+10.39		0.389	.083		
									+13.49	1.23	1.243	.012		
48	39.7+1.5	1423.9	0.48	0.164	1.805	.011	73	29	-16.56	1.35	1.723	.008	- 60	32
		4860.8			2.015	.007			-14.97		1.246	.023	- 259	52
									-13.88		0.926	.047	116	27
									-12.70		0.830	.059	- 216	62
									-11.09		0.659	.088	73	27
									+10.99		0.481	.135	7	21
									+14.58		1.637	.009	- 66	30
									+16.07		1.871	.006	28	16
49	39.9-0.0	823.1	0.37	0.159	0.946	.025	139	33	-14.66	2.60	0.687	.028	130	38
		5159.1			1.023	.021			-13.66		0.557	.038	1547	71
									-11.83		0.359	.060	83	74
									+10.34	1.28	0.107	.109	728	86
									+12.03		0.226	.082	1122	139
									+13.20		0.438	.050	9	96
									+14.69	1.17	0.965	.015	141	49
50	42.3-0.1	1944.6	0.48	0.072	1.234	.020	- 630	149	-16.15	1.02	0.840	.030	- 466	185
		5080.2			1.511	.012			-15.03		0.592	.053	- 710	195
									-14.21		0.525	.062	- 652	165
									-11.65		0.376	.088	- 557	184
									-10.63		0.389	.086	-1250	313
									- 9.31	2.76	0.534	.061	- 572	194
									+11.45	1.81	0.582	.055	-2834	190
									+13.21		0.597	.053	- 564	196
									+16.67	1.38	1.448	.008	- 539	186
51	44.8-2.3	551.7	0.34	0.155	0.945	.027	129	48	-16.17	1.36	0.984	.015	- 598	29
		5064.1			1.172	.016			-13.44	1.04	0.194	.095	- 394	75
									+16.00	1.02	1.353	.007	164	53
52	45.5+0.1	760.5	0.31	0.185	0.875	.037	198	17	-17.12	1.52	0.884	.021	1	7
		4946.6			0.834	.040			+17.61	0.88	0.975	.017	277	15
53	51.8-0.2	(1162)	(0.41)	0.033	0.970	.023			-19.39	1.61	0.855	.017		
		(4998.2)			0.851	.030			-17.44		0.456	.041		
									-15.96		0.194	.076		
									-13.62	1.27	-0.069	.142		
									+16.65		0.160	.082		
									+18.34	2.02	0.644	.027		
									+19.59		0.370	.050		
54	53.6-0.2	(838)	(0.44)	0.023	0.980	.030			-13.16	2.04	0.917	.023		
		(4816.4)			1.346	.013			+ 9.98		0.351	.084		
									+11.85		0.730	.035		
									+13.86	0.89	1.442	.007		
55	75.3-1.8	1602.7:	0.39	0.215	0.939	.020	546	53	-12.54		0.861	.017	- 222	29
		4481.2			0.892	.022			-11.69	1.71	0.903	.015	- 390	42
									-10.50		0.297	.061	- 153	45
									- 9.55	0.79	0.183	.080	-1517	80
									+ 9.39		0.286	.063	622	79
									+10.41		0.524	.036	526	61
									+11.43	0.95	0.866	.017	393	39
56	77.9+0.2	(1339)	(0.41)	0.039	0.944	.022			-11.41	0.81	0.828	.021		
		(4939.4)			0.867	.026			-10.31	0.92	1.024	.013		
									+ 8.65	0.86	-0.007	.145		

TABLE III *(continued)*.

	Name	P_R JD$_o$ (Days)	f_R	m_l	Log $\bar{S}_{LV}$ m.e. Log $\bar{S}_{HV}$ (1σ) (Log 10^{-22} Wm^{-2})	$\Delta\phi$(HV-LV)	±	v_k-v_* (km s^{-1})	fw_k (km s^{-1})	Log $\bar{S}_k$ (Log Jy)	m.e.$_k$ (1σ)	$\Delta\phi_k$ (10^{-4})	±
								+ 9.57		0.310	.068		
								+11.51	1.55	0.871	.019		
57	83.4-0.9	1153.0	0.50	0.255	0.994 .022	- 185	9	-17.99	1.21	1.071	.010	233	14
		4996.8			0.508 .066			-13.81	2.40	-0.003	.125	- 229	14
								+16.46		0.145	.088	- 81	7
								+17.44	2.17	0.245	.069	- 390	24
								+18.15	2.13	0.344	.055	298	16
58	104.9+2.4	1215.0:	0.50	0.133	1.854 .004	216	26	-14.81	1.91	1.646	.004	- 191	23
		4880.9			1.741 .005			-13.79		1.494	.005	- 17	27
								-12.78		1.248	.009	53	24
								-11.23		1.157	.011	- 30	17
								- 8.09		0.488	.052	- 259	45
								- 6.44		0.415	.062	- 99	29
								+ 7.14		0.235	.094	886	41
								+ 9.72		0.525	.048	187	29
								+10.88		0.690	.033	- 26	23
								+13.48		1.206	.010	237	28
								+15.27	1.53	1.622	.004	151	31
59	127.9-0.0	1994.1:	0.49	0.294	1.904 .003	379	18	-10.78	0.86	2.050	.002	- 123	15
		5765.4			1.640 .005			- 9.65		1.279	.008	116	40
								- 8.63	0.83	1.002	.016	668	24
								+10.19		1.284	.008	452	27
								+11.21	2.52	1.383	.007	582	25
60	138.0+7.2	1352.1:	0.35	0.161	1.108 .014	188	57	- 9.26		1.267	.008	177	76
		5376.3			0.938 .021			- 7.37		0.512	.043	- 232	47
								+ 8.33		0.448	.050	465	66
								+ 9.63		1.150	.010	258	57

TABLE IVa. — *Mira variables and M-type supergiants.*

	Name	Δm_r (mag)	v_e (km s^{-1})	$\delta\phi$	f_c	R_p (10^{16} cm.)	ΔR_p	R_i' (10^{16} cm.)	$\Delta R_i'$	R_o (10^{16} cm.)	ΔR_o	Remarks
1	R Aql	0.87	6.815	.012	.777	2.37	0.99	0.57	0.32	0.74	0.41	
2	RR Aql	0.71	6.235	.013	.837	0.28	0.23	0.29	0.18	0.29	0.20	
3	SY Aql	0.62	4.375	.009	.694	2.88	1.84	-1.75	1.84	0.57	2.32	Poor baselines
7	Z Cyg	0.70	2.120	.009	.708	0.42	0.76	0.23	0.49	0.29	0.58	
8	U Ori	0.94:	3.050	.011	.753	3.33:	1.86	3.54:	0.80	3.51:	1.06	Flux decreasing
9	WX Psc	1.16	17.910	.014	.810	2.55	0.08	3.14	0.05	2.97	0.06	IRC+10011
10	WX Ser	0.58	7.585	.009	.784	-1.02	1.19	-1.59	0.56	<0.17		
11	IK Tau	1.33	16.730	.012	.788	-0.14	0.13	0.40	0.18	0.13	0.17	
12	RS Vir	0.48	4.285	.008	.722	0.47	0.73	1.01	0.51	0.46	0.86	
4	VY CMa	0.18	35.900	.007	.755	-8.83	1.16	-3.17	0.94	-5.41	1.33	
5	PZ Cas	0.29	28.890	.016	.772	1.04	1.06	3.27	1.99	1.53	1.45	
6	NML Cyg	0.31	25.575	.006	.765	-0.63	0.24	-4.57	0.92	-0.88	0.33	

TABLE IVb. — *OH/IR stars with large amplitudes ($\Delta m > 0.60$).*

	Name OH———	Δm_r (mag)	v_e (km s^{-1})	$\delta\phi$	f_c	R_p (10^{16} cm)	ΔR_p	R_i' (10^{16} cm)	$\Delta R_i'$	R_o (10^{16} cm)	ΔR_o	Remarks
28	20.2-0.1	0.67	16.445	.029	.801	2.27	2.98			2.27	2.98	Confusion
29	20.7+0.1	0.99	18.210	.017	.806	10.26	0.92			10.26	0.92	Confusion
30	21.5+0.5	1.09	18.760	.017	.800	16.33	0.87			16.33	0.87	Confusion
32	26.2-0.6	1.05	22.115	.019	.803	- 0.11	0.24	0.19	0.13	0.12	0.14	
34	26.5+0.6	1.13	14.070	.014	.792	3.10	0.22	4.82	0.62	3.29	0.26	
36	28.5-0.0	0.77	13.120	.038	.793	0.02	0.19	1.10	0.47	0.17	1.51	
37	28.7-0.6	0.83	17.380	.029	.801	1.48	0.29	- 0.13	0.43	0.98	1.81	
39	30.1-0.2	0.81	17.600	.032	.812	0.90	0.33			0.90	0.33	Confusion
43	32.0-0.5	0.88	20.575	.028	.814	7.47	2.08	7.41	0.83	7.42	1.09	
44	32.8-0.3	1.24	16.385	.013	.764	11.52	0.50	17.33	0.21	16.46	0.33	
45	35.6-0.3	0.78	13.520	.028	.808	4.56	1.16	3.80	3.30	4.48	1.68	
48	39.7+1.5	0.82	16.580	.019	.813	1.73	0.38	1.66	0.66	1.71	0.47	
49	39.9-0.0	0.80	14.710	.026	.822	- 2.04	1.57	1.80	0.43	1.53	0.53	
51	44.8-2.3	0.77	15.855	.036	.809	5.34	0.18	1.14	0.42	4.69	0.70	
52	45.5+0.1	0.92	17.125	.032	.828	2.68	0.11	2.36	0.20	2.61	0.14	
55	75.3-1.8	1.08	12.025	.028	.891	16.00	1.63	12.73	1.24	13.93	1.38	
57	83.4-0.9	1.28	18.110	.008	.822	0.97	0.22			0.97	0.22	Poor baselines
58	104.9+2.4	0.66	14.915	.012	.799	4.42	0.36	4.26	0.51	4.37	0.42	
59	127.9-0.0	1.47	10.975	.012	.791	17.06	1.75	12.38	0.59	12.86	0.72	
60	138.0+7.2	0.81	9.365	.013	.795	3.13	1.98	4.14	1.26	3.85	1.64	

TABLE IVc. — *OH/IR stars with intermediate amplitudes (0.30 < Δm < 0.60).*

	Name OH———	Δm_r (mag)	v_e (km s^{-1})	δφ	f_c	R_p (10^{16} cm)	ΔR_p	R'_i (10^{16} cm)	$\Delta R'_i$	R_o (10^{16} cm)	ΔR_o	Remarks
6	80.8-1.9	0.31	25.575	.006	.765	-0.63	0.24	- 4.57	0.92	-0.88	0.33	NML Cyg
17	12.3-0.2	0.56	13.830	.034	.793	-1.63	1.12			-1.63	1.12	Confusion
18	12.8-1.9	0.56	22.615	.037	.761	3.72	1.17	1.88	0.53	2.19	0.63	
19	12.8+0.9	0.34	11.080	.031	.785							Absorption in spectru
20	13.1+5.0	0.53	15.670	.037	.787	7.82	0.23	10.79	0.64	8.16	0.28	
22	16.1-0.3	0.55	22.075	.030	.809	1.50	0.34	2.53	0.86	1.64	0.40	
23	17.4-0.3	0.59	16.830	.032	.801	0.31	3.65			0.31	3.65	Confusion
33	26.4-1.9	0.44	12.085	.030	.792	0.12	2.88	<0.89	1.57	<0.71		
35	27.3+0.2	0.59	12.830	.043	.801	-1.25	1.40			<0.15		Confusion
38	30.1-0.7	0.40	20.510	.018	.805	3.40	0.52	4.05	0.90	3.56	0.62	
40	30.7+0.4	0.57	17.240	.019	.795	9.18	3.39			9.18	3.39	Confusion; Peaks 5-8 dubious
46	36.9+1.3	0.56	7.325	.012	.777	-0.33	0.74	0.32	0.20	0.28	0.23	Weak; S_{HARM} < 4 Jy
50	42.3-0.1	0.36	16.370	.019	.795	-2.37	4.50			<2.13		Confusion? Bad baselines

TABLE IVd. — *OH/IR stars with small amplitudes (Δm < 0.30).*

	Name OH———	Δm_r (mag)	v_e (km s^{-1})	δφ	f_c	R_p (10^{16} cm)	ΔR_p	R'_i (10^{16} cm)	$\Delta R'_i$	R_o (10^{16} cm)	ΔR_o	Remarks
16	11.5+0.1	0.23	29.390	.029	.755	0.60	0.60			0.60	0.60	Confusion
24	17.7-2.0	0.16	12.890	.021	.767	- 3.38	0.95	-4.51	2.00	- 3.59	1.14	
25	18.3+0.4	0.27	15.055	.032	.794	12.72	6.25			12.72	6.25	Confusion
26	18.5+1.4	0.19	10.850	.010	.757	< 0.49	2.24	1.83	3.10	< 0.95		
27	18.8+0.3	0.26	14.660	.029	.828	< 0.39	1.34	-0.95	0.55	< 0.39		
31	25.1-0.3	0.21	12.140	.029	.796	0.95	0.26	0.36	0.68	0.87	0.63	Confusion
42	31.0+0.0	0.21	7.640	.009	.764	1.70	1.11			1.70	1.11	W43A; Confusion

TABLE IVe. — *OH/IR stars without recognizable variation.*

	Name OH———	Δm_r (mag)	v_e (km s^{-1})	δφ	Remarks
13	359.4-1.3	0.13	16.605	.033	Low S/N
14	0.3-0.2	0.16	15.540	.032	Low S/N
15	1.5-0.0	0.21	13.085	.033	
21	15.7+0.8	0.13	14.705	.033	
41	31.0-0.2	0.13	14.270	.030	Confusion
47	37.1-0.8	0.13	13.585	.027	
53	51.8-0.2	0.16	19.335	.032	
54	53.6-0.2	0.12	13.340	.036	
56	77.9+0.2	0.19	11.045	.029	

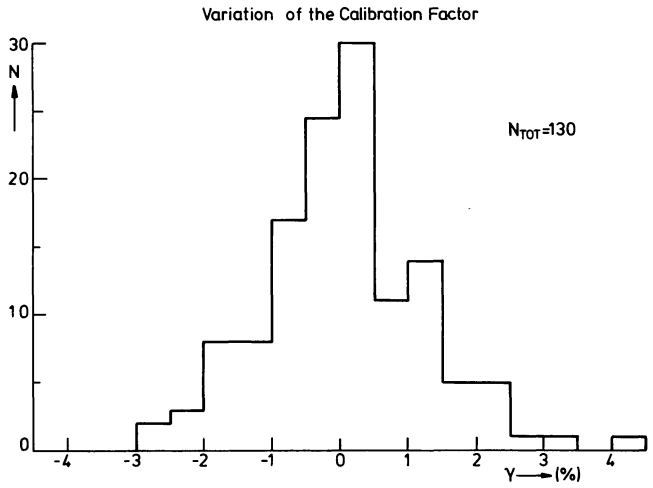

FIGURE 1. — Variation of the noisestep, NS, on subsequent days i and $(i + 1)$. $\gamma = \dfrac{NS(i + 1) - NS(i)}{NS(i)}$.

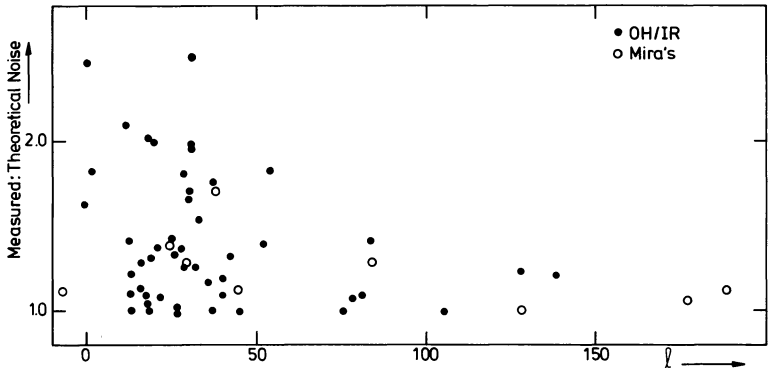

FIGURE 2. — Ratio of the noise measured in the spectra to the noise expected from equation (1) as a function of galactic longitude.

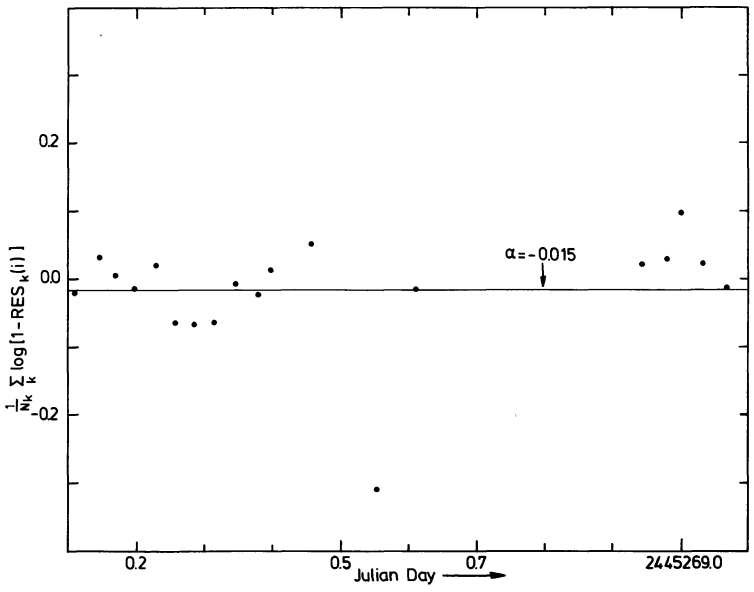

FIGURE 3. — Mean residuals with respect to the sinewave fit for 19 sources observed around a calibration measurement at JD = 244 5268.8. Here N_k denotes the number of peaks of each star.

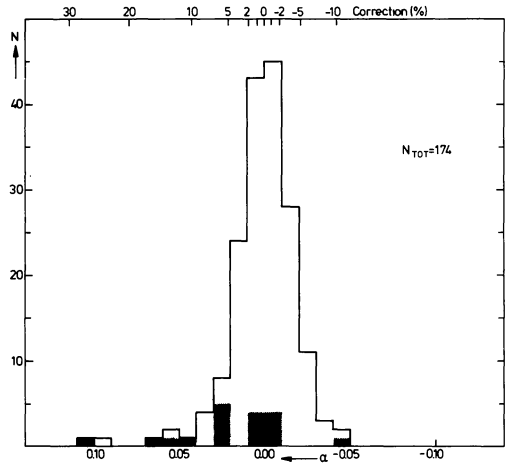

FIGURE 4. — Histogram of α-values for calibration intervals with $N > 10$. Days where no calibration measurement was done are shaded.

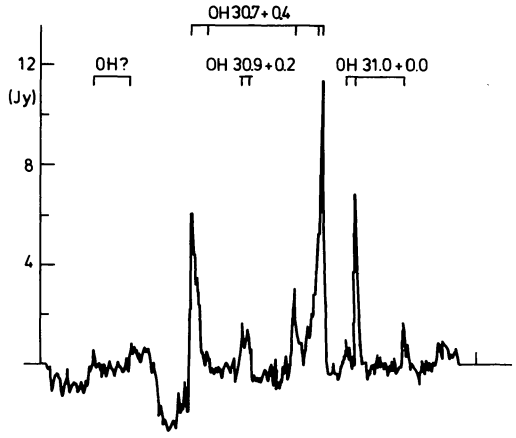

FIGURE 5. — Single-dish profile of the star OH 30.7 + 0.4. In the middle of the spectrum two peaks of OH 30.9 + 0.2 can be seen, and at the right (LV) side another star OH 31.0 + 0.0. At the high velocity side strong and broad absorption is always present and sometimes also two peaks of an unknown, variable OH-source. This is one of the worst examples of confusion.

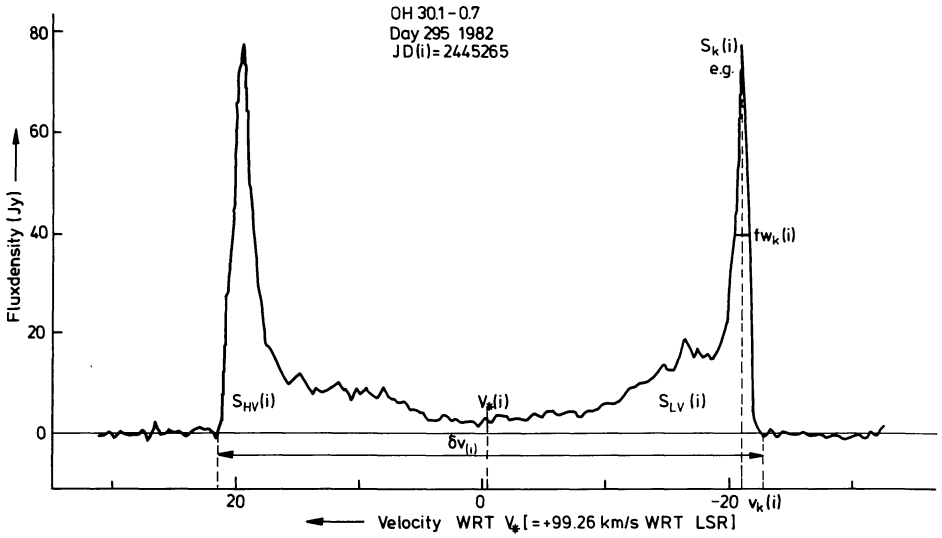

FIGURE 6. — Single-dish profile of OH 30.1 − 0.7. The quantities that are measured in the monitor program are indicated.

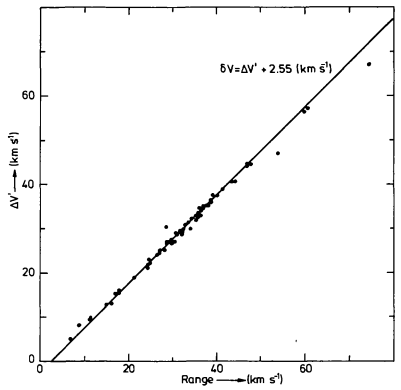

FIGURE 7a. — Comparison between the total range of OH emission (δv) and the velocity separation of the outermost peaks (Δv).

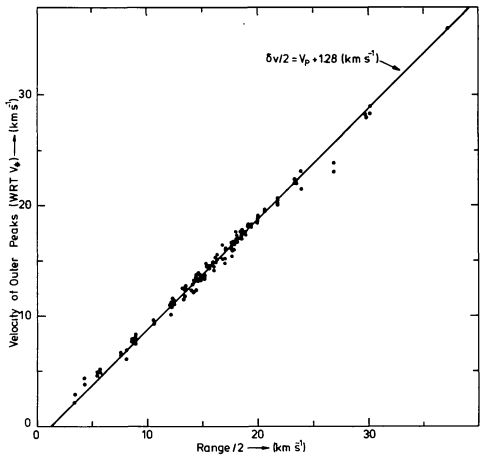

FIGURE 7b. — Comparison of $\delta v/2$ and v_p, the velocity of the outermost peak.

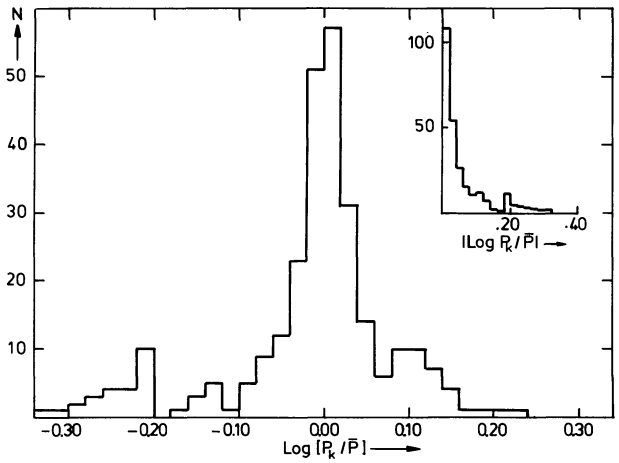

FIGURE 8a. — Distribution of the periods for various peaks (k), normalized to the mean value $\overline{P}$ of a given source, for all *variable* OH/IR stars. Note the second maximum at − 0.20, caused by some weak peaks with less phase coverage than the others, through which the sinewave fits with half the main period.

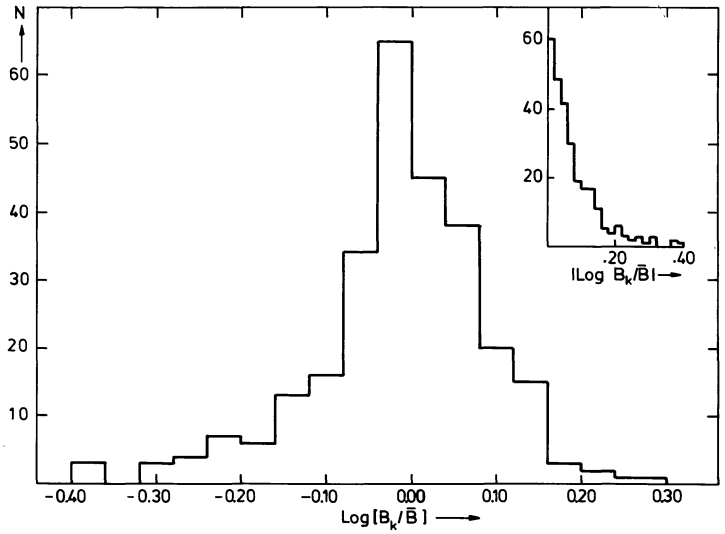

FIGURE 8b. — Distribution of the amplitudes for various peaks, normalized as in figure 9a. $B_k = b_k/a_k$, and $\overline{B}$ is the mean (relative) amplitude for a given star.

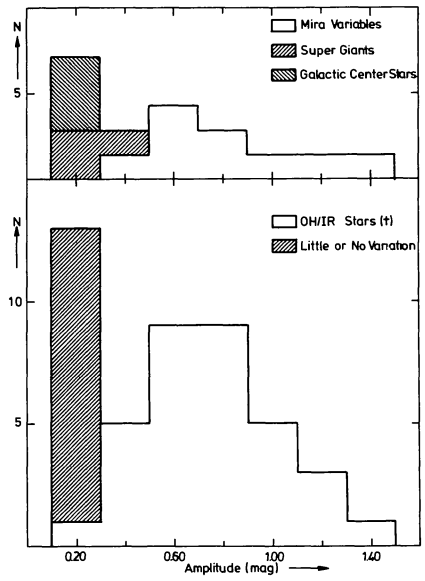

FIGURE 9. — Amplitude distribution of all 60 stars included in the monitor program. The supergiants have extreme Δv's, the non-variable OH/IR stars normal ones.

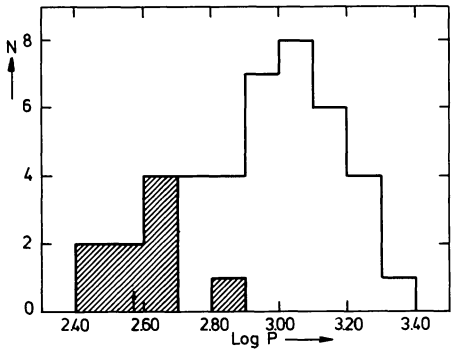

FIGURE 10. — Period distribution for the variable OH/IR stars and for the OH-Mira's (shaded). The arrow marks the mean period for Mira variables (Wood and Cahn, 1977).

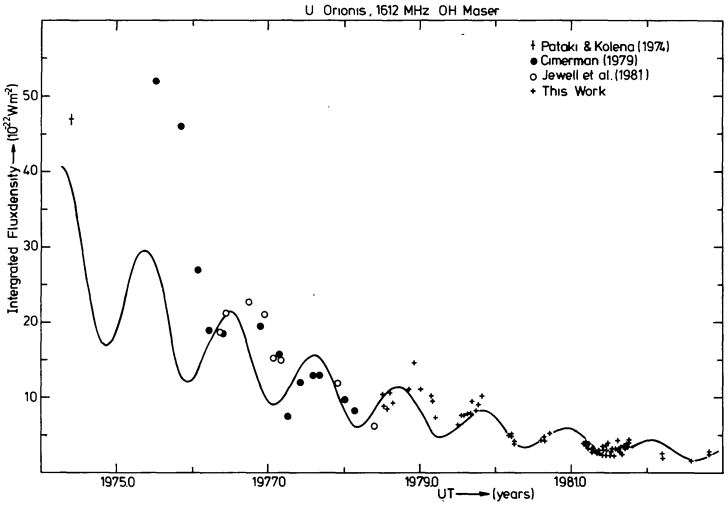

FIGURE 11. — Total flux of U Ori at 1612 MHz. Before 1974 it could only be seen in the main lines.

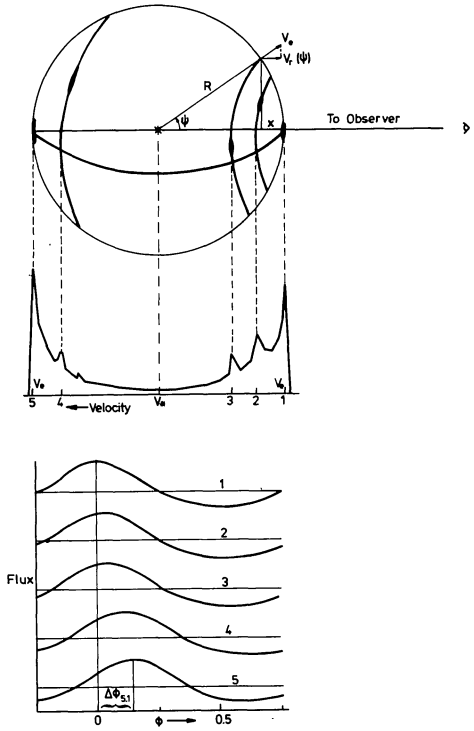

FIGURE 13. — Schematic representation of the uniformly expanding OH shell, the resulting single-dish spectrum, and the variations of different parts in the spectrum.

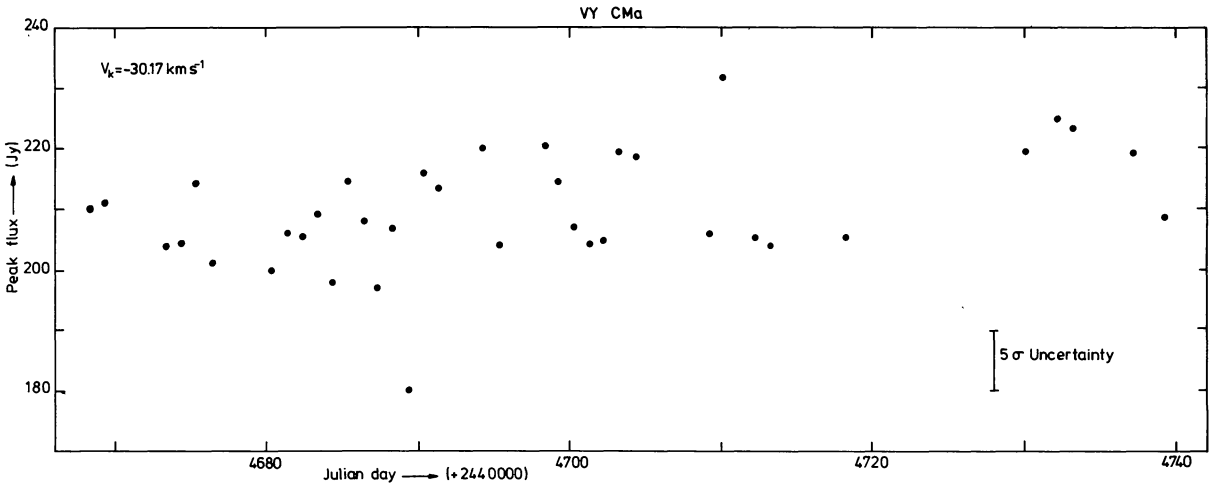

FIGURE 12. — Short term variation of the strongest feature in the spectrum of VY CMa. This star was observed almost daily over a stretch of 200 days. A Fourier analysis reveals a main period of $\sim$ 1000 days, an intermediate time scale of $\sim$ 180 days, and short term variations of $\lesssim$ 2 days.

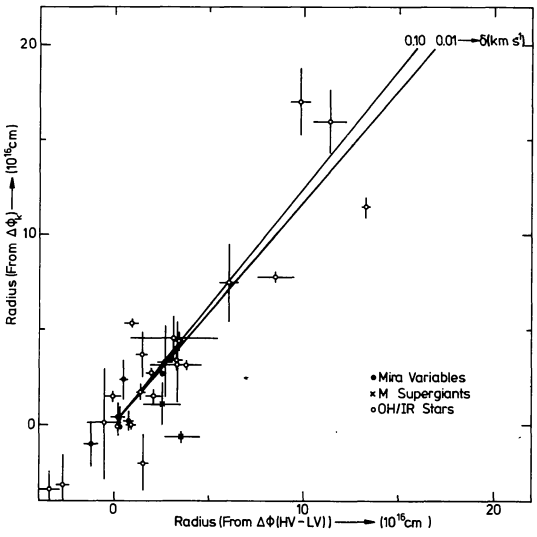

FIGURE 14. — Comparison of the radii determined from the phase lags between the curves of the integrated flux densities and of the peak flux densities. The drawn lines are the expected relation for the model case; δ = 0.10 and 0.01 km s^{-1} corresponds to f_c = 0.79 and 0.85 respectively.

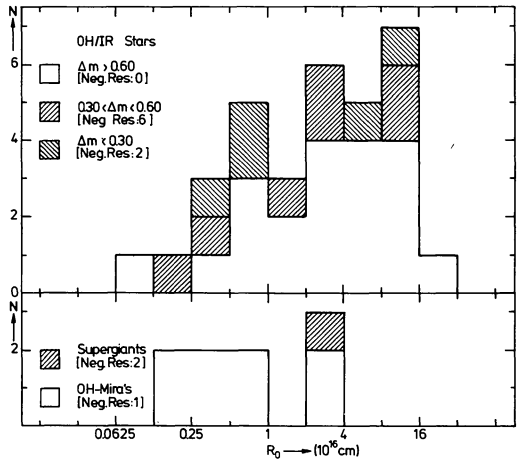

FIGURE 15. — Distribution of the radii (R_0) for all variable stars in the program. The number of negative results for each group is given in brackets.

Appendix A. — RADIO LIGHT CURVES OF OH MASERS.

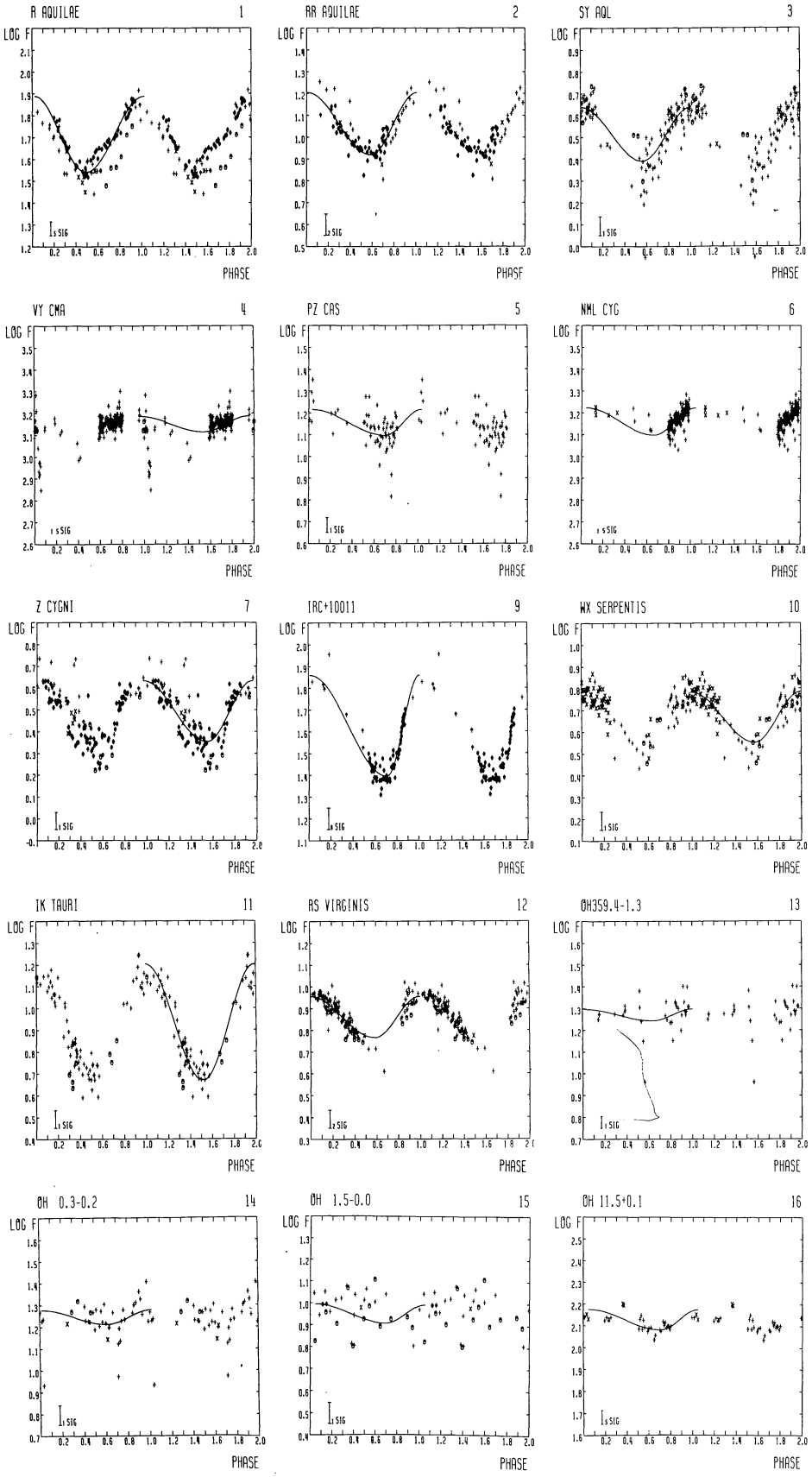

(continued).

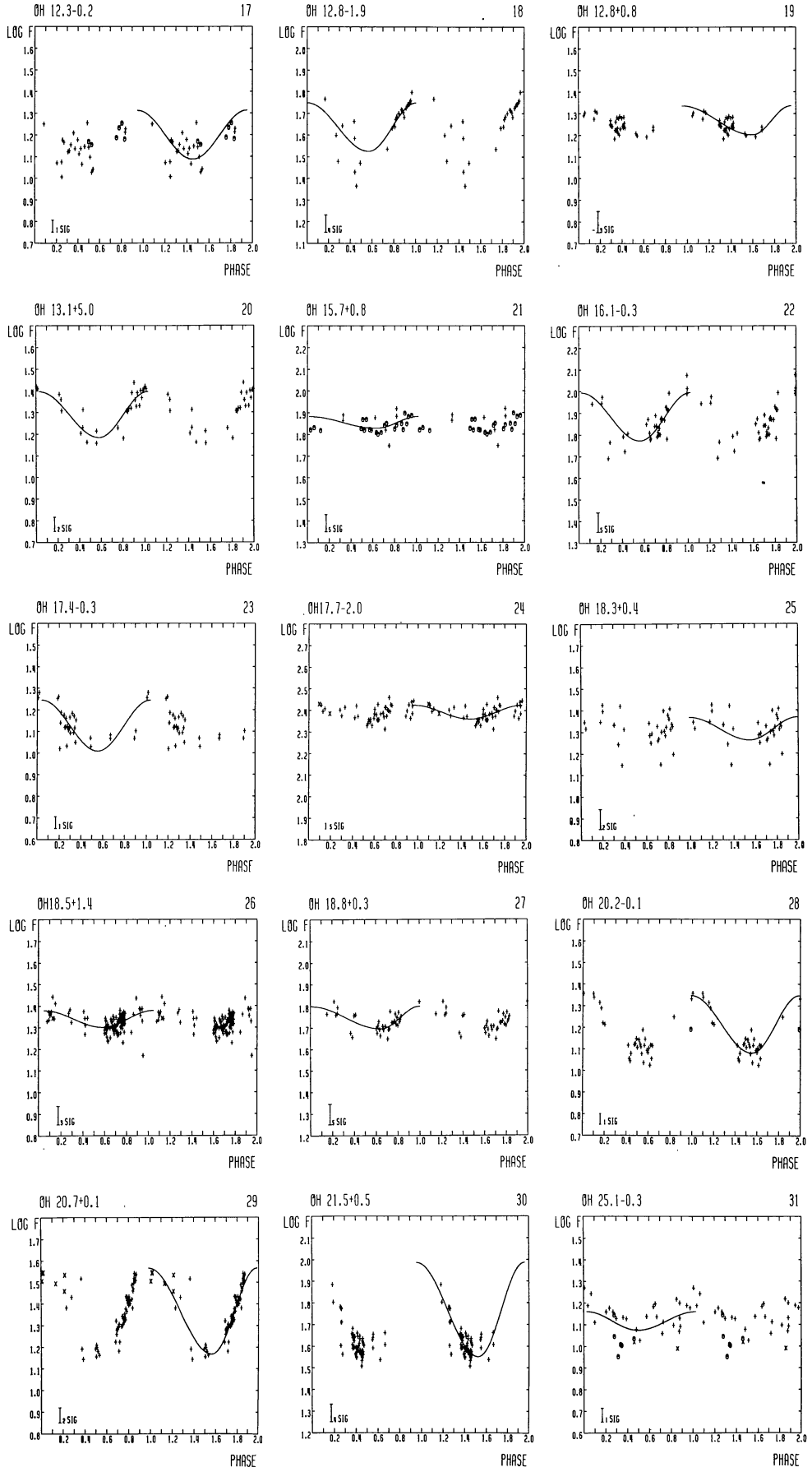

(continued).

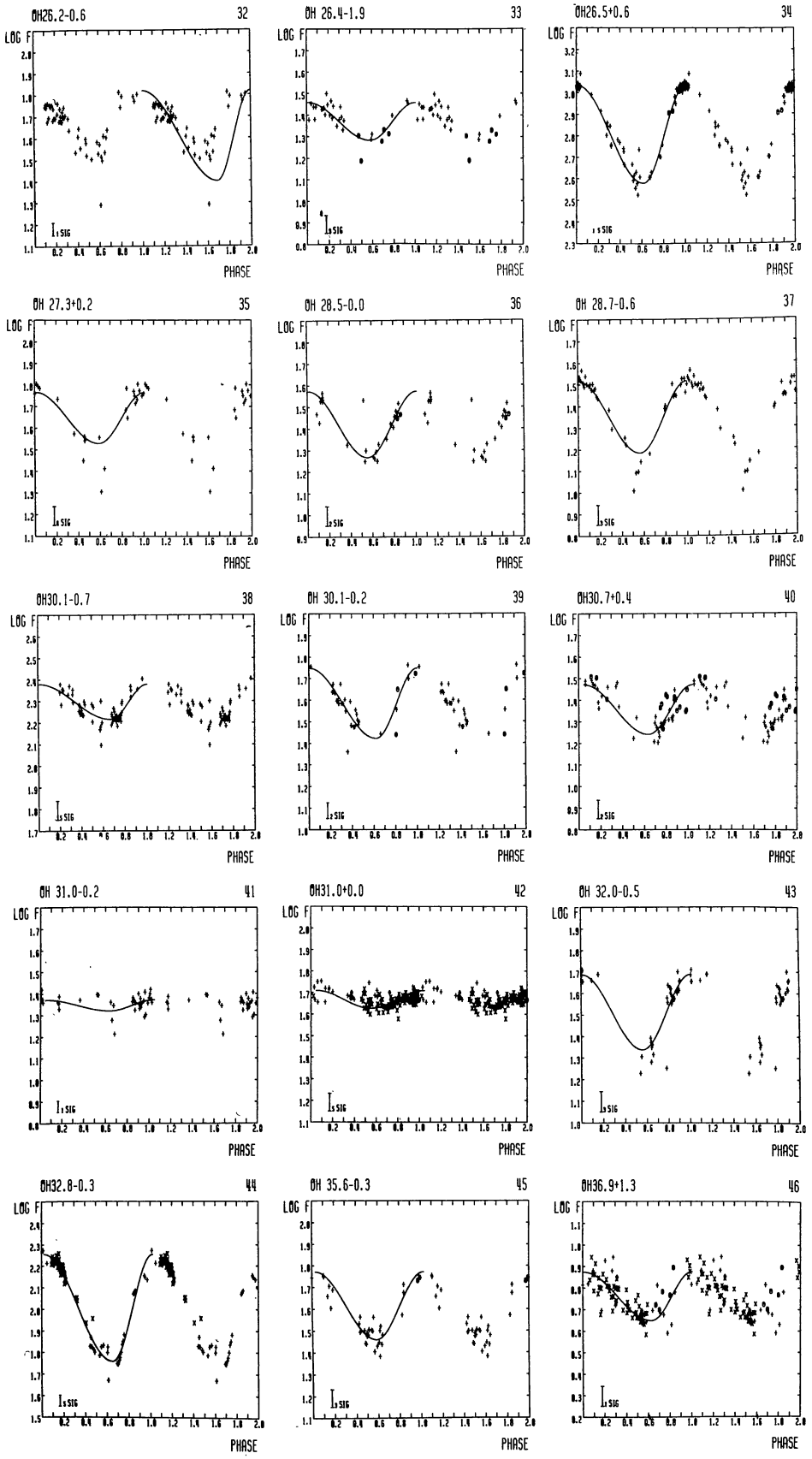

(continued).

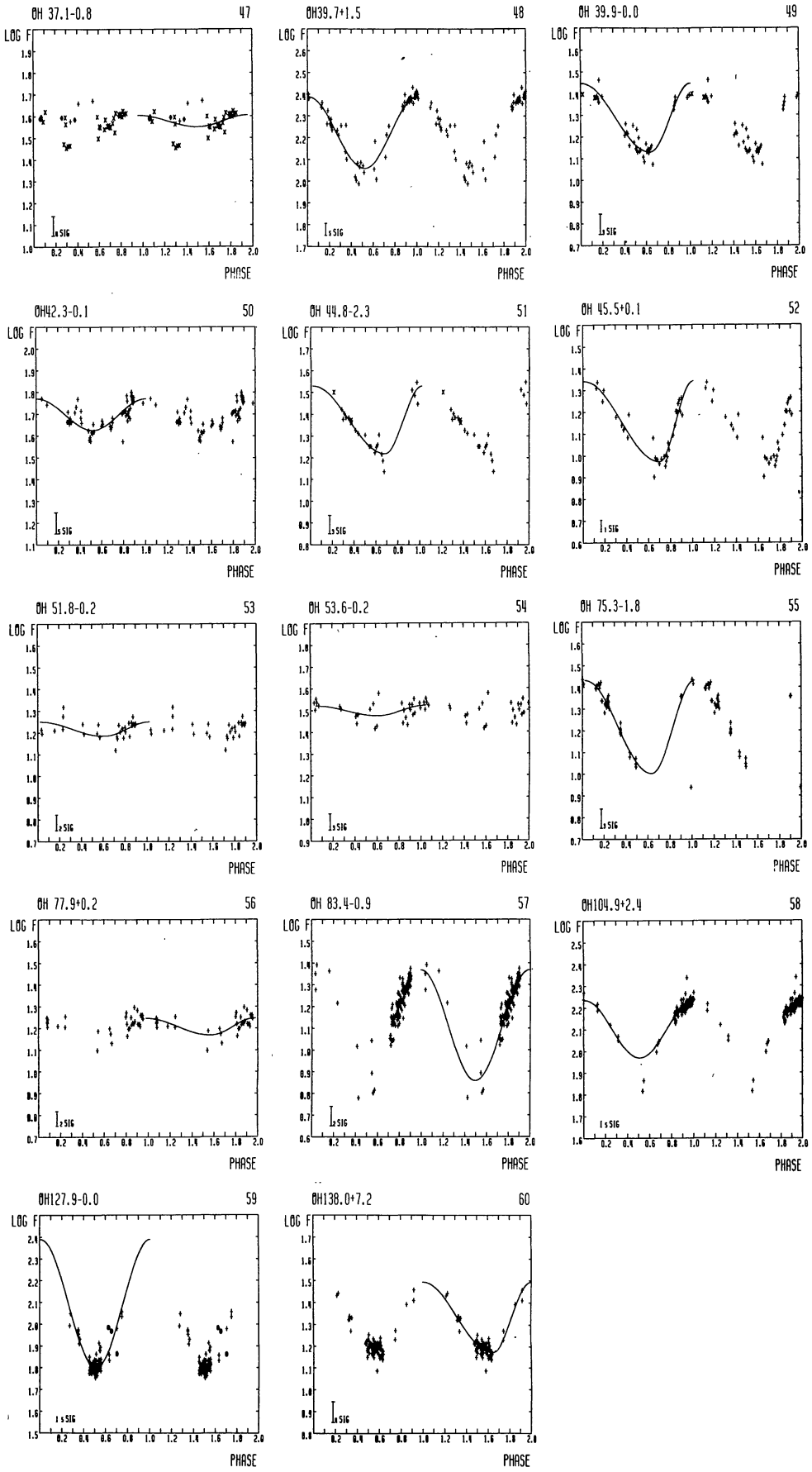

Appendix B. — Phase lag as a function of velocity.

a. *Mira variables and M-type supergiants.*

Figures 1 to 12.

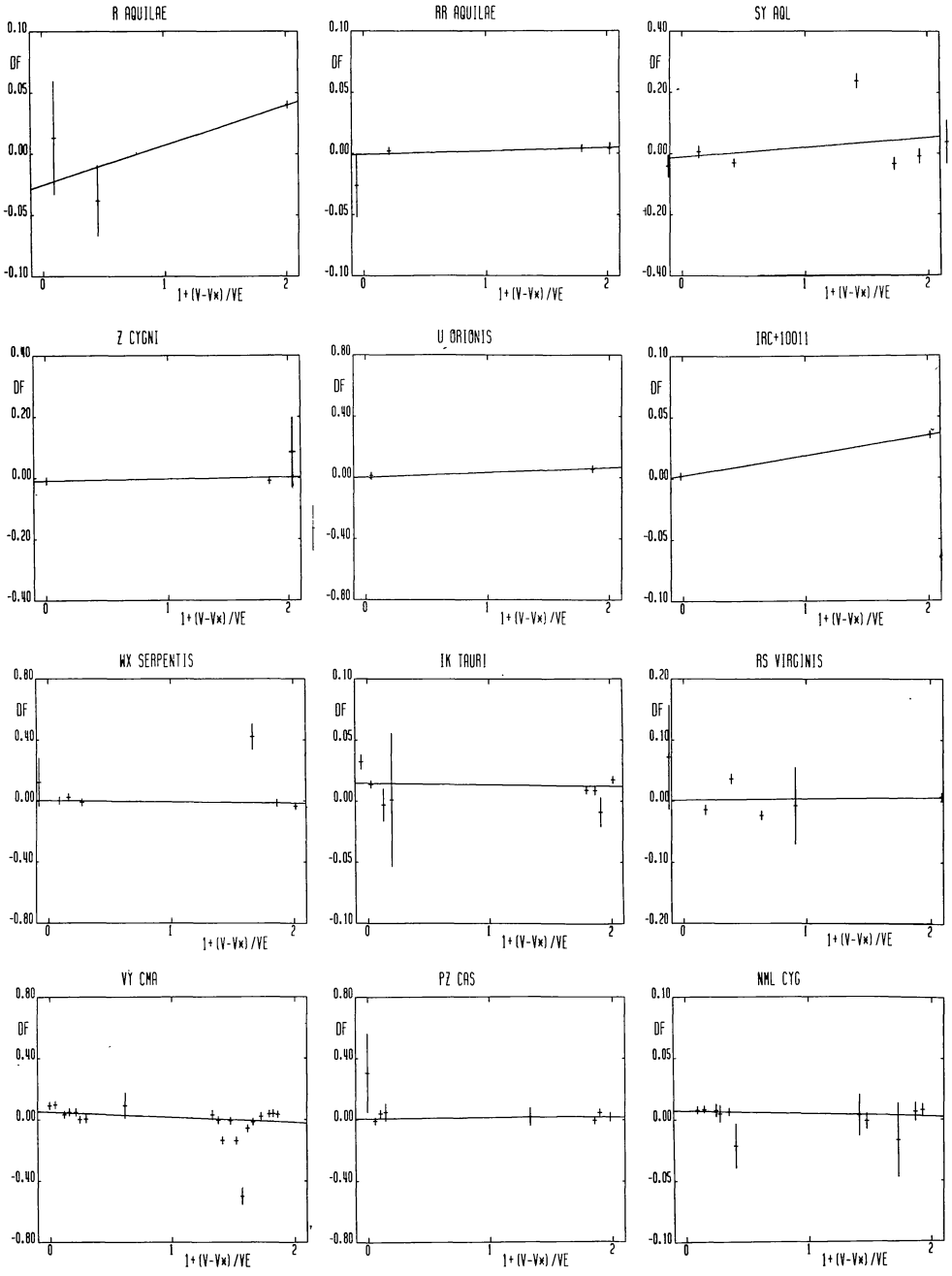

b. *OH/IR stars with large amplitude ($\Delta m_r > 0^m.60$).*

FIGURES 13 to 32.

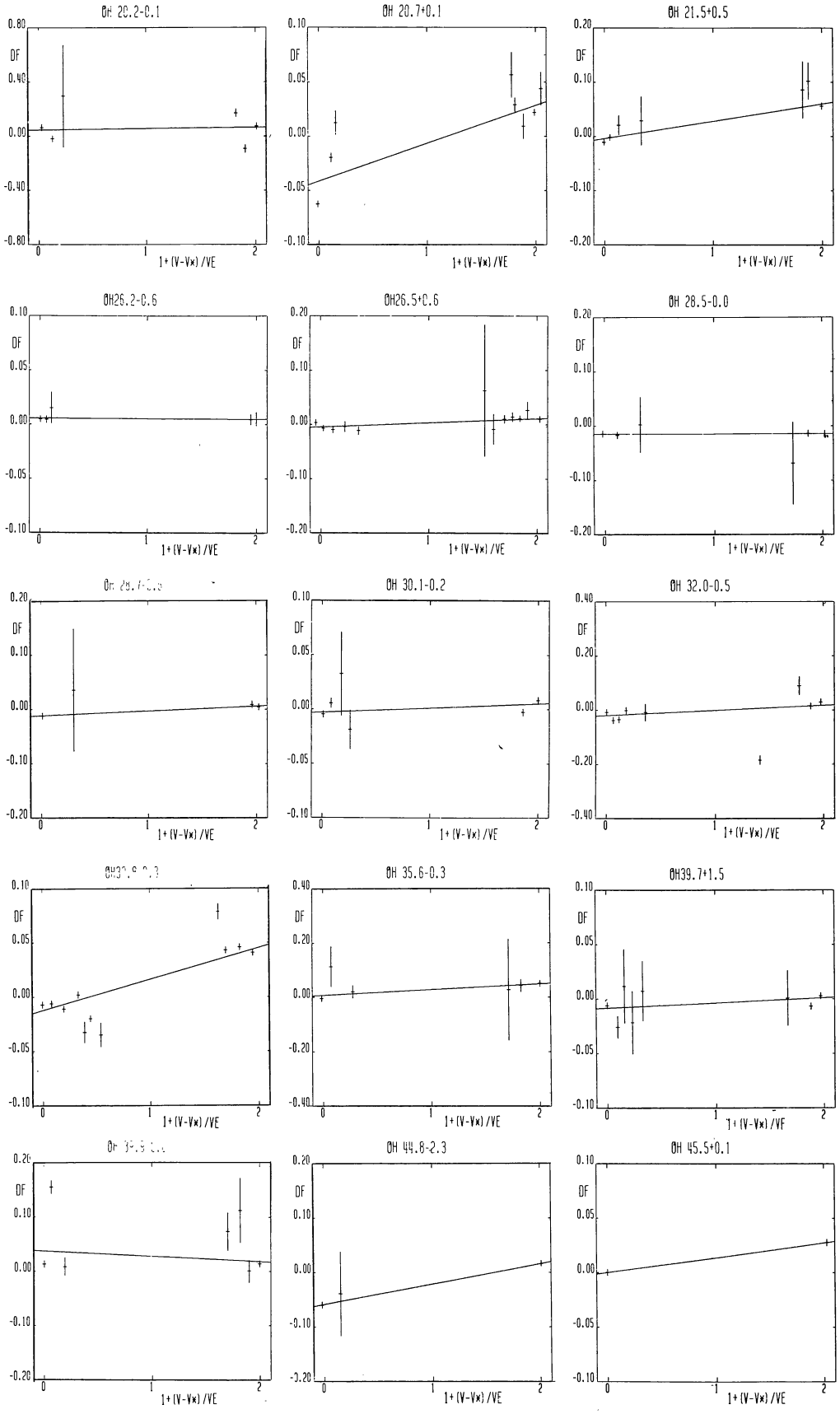

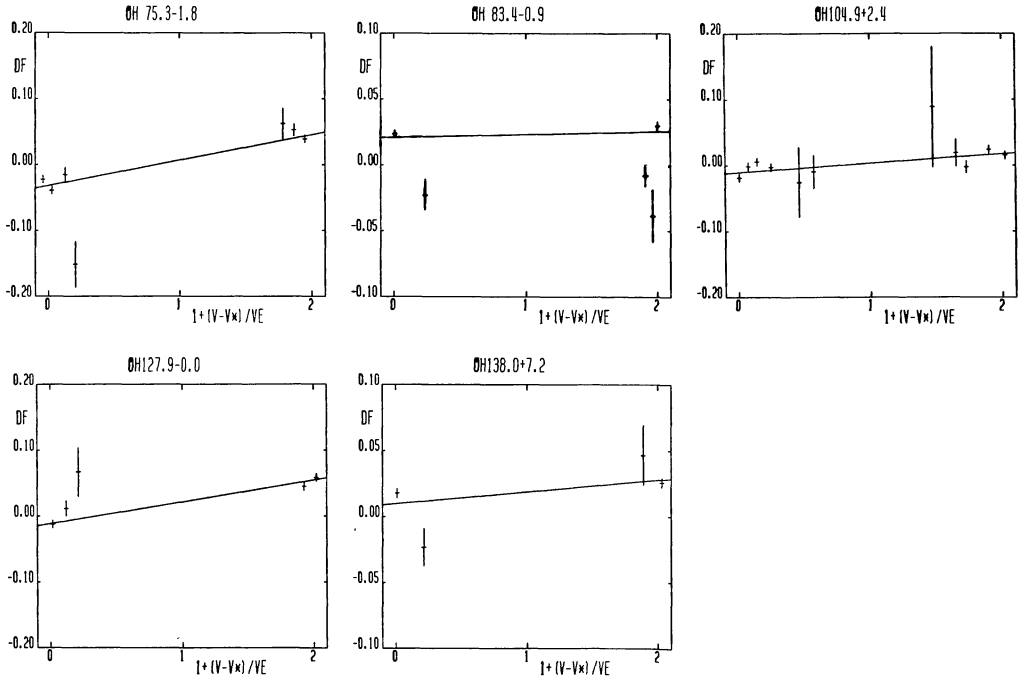

c. *OH/IR stars with intermediate amplitude ($0^m.30 < \Delta m_r < 0^m.60$).*

FIGURES 33 to 44.

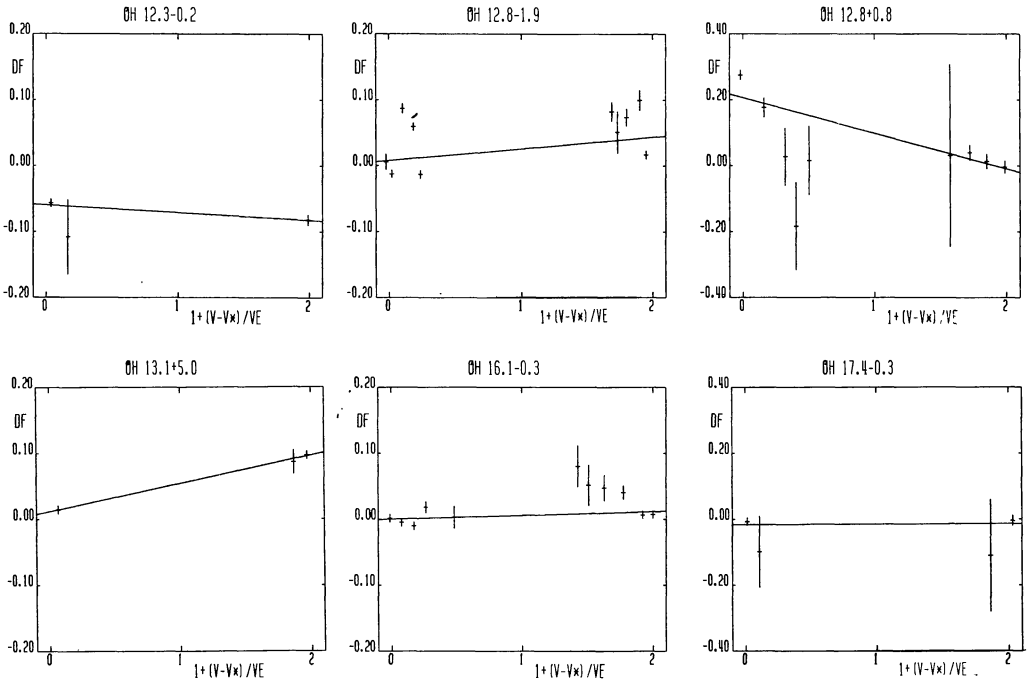

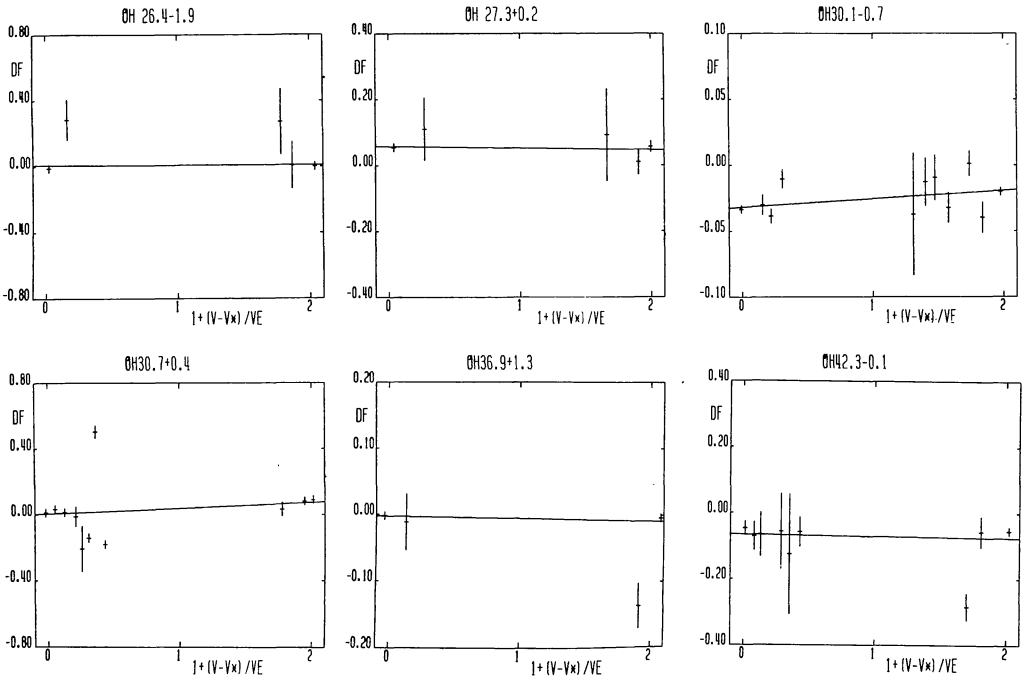

d. *OH/IR stars with small amplitudes ($\Delta m_r < 0^m.30$).* FIGURES 45 to 51.